



University of North Dakota  
UND Scholarly Commons

---

Theses and Dissertations

Theses, Dissertations, and Senior Projects

---

January 2018

# Seperation Of Fuel-Based Contaminents From Oxygen Carriers In Chemical Looping Combustion

Benjamin Robert Jensen

Follow this and additional works at: <https://commons.und.edu/theses>

---

## Recommended Citation

Jensen, Benjamin Robert, "Seperation Of Fuel-Based Contaminents From Oxygen Carriers In Chemical Looping Combustion" (2018). *Theses and Dissertations*. 2412.  
<https://commons.und.edu/theses/2412>

This Thesis is brought to you for free and open access by the Theses, Dissertations, and Senior Projects at UND Scholarly Commons. It has been accepted for inclusion in Theses and Dissertations by an authorized administrator of UND Scholarly Commons. For more information, please contact [zeinebyousif@library.und.edu](mailto:zeinebyousif@library.und.edu).

SEPERATION OF FUEL-BASED CONTAMINENTS FROM OXYGEN CARRIERS IN  
CHEMICAL LOOPING COMBUSTION

By

Benjamin Robert Jensen  
Bachelor of Science, University of North Dakota, 2017

A Thesis  
Submitted to the Graduate Faculty

of the  
University of North Dakota  
in partial fulfillment of the requirements

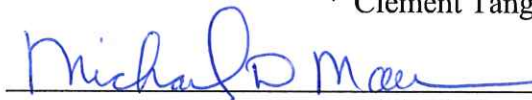
for the degree of  
Master of Science

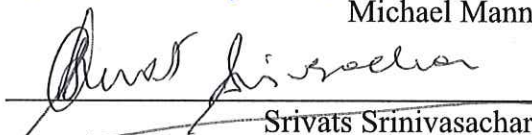
Grand Forks, North Dakota

December  
2018

This thesis, submitted by Benjamin Robert Jensen in partial fulfillment of the requirements for the Degree of Master of Science from the University of North Dakota, has been read by the Faculty Advisory Committee under whom the work has been done and is hereby approved.

  
Clement Tang

  
Michael Mann

  
Srivats Srinivasachar

This thesis is being submitted by the appointed advisory committee as having met all the requirements of the School of Graduate Studies at the University of North Dakota and is hereby Approved.

  
Grant McGimpsey  
Dean of the School of Graduate Studies

  
Date

## PERMISSION

Title            Separation of Fuel-Based Contaminants from Oxygen Carriers in Chemical Looping Combustion

Department    Mechanical Engineering

Degree           Masters of Science

In presenting this thesis in partial fulfillment of the requirements for a graduate degree from the University of North Dakota, I agree that the library of this University shall make it freely available for inspection. I further agree that permission for extensive copying for scholarly purposes may be granted by the professor who supervised my thesis work or, in her (or his) absence, by the Chairperson of the department or the dean of the School of Graduate Studies. It is understood that any copying or publication or other use of this thesis or part thereof for financial gain shall not be allowed without my written permission. It is also understood that due recognition shall be given to me and to the University of North Dakota in any scholarly use which may be made of any material in my thesis.

Benjamin Robert Jensen  
11/26/18

## TABLE OF CONTENTS

LIST OF FIGURES .....	vii
LIST OF TABLES .....	ix
ACKNOWLEDGMENTS .....	x
ABSTRACT.....	xi
CHAPTER I INTRODUCTION.....	1
Chemical Looping Combustion.....	1
The Problem .....	3
Oxygen Carriers (OC) .....	3
Copper-Based Materials.....	3
Iron-based Materials .....	4
Calcium-based Materials .....	5
Manganese-based Materials.....	6
Attrition and its impacts on char/oxygen carrier separation .....	6
Current Char/OC Segregation Methods .....	7
The Solution .....	9
Size segregation bed (SSB).....	10

Elutriation bed (EB).....	10
Project Objective.....	11
Approach.....	11
CHAPTER II PROOF OF CONCEPT .....	13
CHAPTER III DESIGN AND CONTRUCTION .....	15
Preparation of Test Materials .....	15
Loop Seal Design .....	19
Design and Construction of the Feed Bed.....	25
Design and Construction of the Elutriation Bed .....	27
Design and Construction of the Size Segregation Bed.....	31
Final Design of PCS System .....	36
Process Control.....	40
CHAPTER IV COMPONENT TESTING OF THE HOT FLOW SYSTEM .....	42
Test 3 – SSB testing with 0.5% char/OC mix .....	42
Test 4 – EB Testing of Test 3 Bottoms .....	46
Test 1 – Optimizing EB Performance .....	47
Test 2 – Optimizing SSB Performance .....	49
Summary of Test Results and Implications for the Hot Flow Design.....	51
Operating Conditions .....	51
Control of Hot Flow Unit.....	51

CHAPTER V HOT FLOW RESULTS AND DISCUSSION .....	53
Challenges and Mitigation Strategies.....	53
Results for Coarse (230 $\mu\text{m}$ ) Ilmenite at $\sim 300^\circ\text{C}$ .....	57
Results for Fine (94 $\mu\text{m}$ ) Ilmenite at $\sim 300^\circ\text{C}$ .....	59
CHAPTER VI FUTURE WORK .....	62
CHAPTER VII CONCLUSIONS.....	63
REFERENCES .....	64

## LIST OF FIGURES

Figure 1. Process Schematic for Chemical Looping Combustion .....	2
Figure 2. Char Separation System .....	10
Figure 3. Change in ilmenite size distribution after 5000 min of redox cycling .....	17
Figure 4. PSD of coarse OC and AC .....	18
Figure 5. PSD of fine OC and AC .....	18
Figure 6. Cold flow loop seal calibration for coarse ilmenite.....	20
Figure 7. 3D cross-section of the original loop seal design (left) and an image of the constructed loop seal (right).....	21
Figure 8. Loop seal calibration using fine ilmenite .....	22
Figure 9. New loop seal configurations to be tested.....	23
Figure 10. New loop seal design testing .....	24
Figure 11. Comparison of new loop seal's sensitivity to gas flow .....	24
Figure 12. Cold flow feed bed (left) and hot flow feed bed system under construction (right) ...	26
Figure 13. Cold flow EB unit (left) and hot flow EB unit with air preheater (right).....	28
Figure 14. Bed pressure response as material is fed and removed from the bed.....	29
Figure 15. Graph showing calculated changes in terminal velocity and minimum fluidization velocity with temperature for ilmenite particles .....	30
Figure 16. Image showing cold flow SSB system .....	32
Figure 17. Image showing SSB cold flow set up with rotameters, loop seals, and feed bed .....	33
Figure 18. Image showing char segregation .....	34



Figure 19. Image showing char building up as bed height rises .....	34
Figure 20. Image showing char concentrating in center of bed due to higher air flow at walls ...	35
Figure 21. Final control schematic and configuration of PCS system.....	37
Figure 22. Cross sectional view of SSB.....	38
Figure 23. Completed hot flow unit.....	39
Figure 24. System Control .....	40
Figure 25. Heater control .....	41
Figure 26. PSD of char and ilmenite used during test 3 .....	43
Figure 27. Graph showing test 3 operation of the SSB bottom loop seal (top) and top discharge (bottom).....	44
Figure 28. Chart showing tops/bottom split (left) and char removal efficiency (right) for Test 3	45
Figure 29. Chart showing tops/bottom split (left) and char removal efficiency (right) for Test 4	47
Figure 30. Total material elutriated and corresponding char removal for Test 1 .....	48
Figure 31. Char removal efficiency as a function of particle size and bed velocity.....	49
Figure 32. Chart showing tops/bottoms split (left) and char removal efficiency (right) for Test 2 .....	50
Figure 33. Char removal for 230 $\mu\text{m}$ OC.....	58
Figure 34. Percent Carbon in each size range.....	59
Figure 35. Char removal for 94 $\mu\text{m}$ OC.....	61

## LIST OF TABLES

Table 1. Change in bulk density for an ilmenite sample cycled for 5000 min .....	16
Table 2. Ilmenite particle size distributions.....	17
Table 3. Carbon content of AC and char for different size bins .....	19
Table 4. Feed bed specification .....	26
Table 5. Specifications for the EB at cold flow conditions and calculated hot flow conditions ..	30
Table 6. Specifications for the SSB cold and hot flow conditions .....	36
Table 7. SSB operating conditions during test 3 of cold flow work.....	43
Table 8. Operating conditions for SSB and EB units .....	51
Table 9. Test Conditions for 230 $\mu\text{m}$ 300°C tests .....	57
Table 10. Test Conditions for 94 $\mu\text{m}$ 300°C tests.....	60

## ACKNOWLEDGMENTS

I am greatly thankful to the Institute for Energy Studies (IES) of UND and Energex LLC for giving me the opportunity to work on my research. I cannot express how thankful I am to the individuals at IES and Energex for their support, guidance, and knowledge that they provided to make this work possible. I would also like to express my gratitude to my previous advisor Dr. Nanak Grewal, current advisor Dr. Clement Tang, and committee members Dr. Michael Mann and Dr. Srivats Srinivasachar for their guidance and review of my thesis report. Lastly, I'd like to thank the United States Department of Energy (DOE) for providing the funding necessary for this research.

## ABSTRACT

This project involved the development of a technology for segregating fuel-based contaminants (char) from oxygen carrier material in the context of chemical looping combustion (CLC) application. In chemical looping, the well-mixed solids that flow from the fuel reactor consisting of char and oxygen carrier particles cannot be completely separated into their constituents before they enter the air reactor. The slip of carbon leads to char oxidation in the wrong reactor and poor carbon dioxide separation efficiency. An efficient method to separate char from oxygen carrier material is critical for the deployment of chemical looping technology. This segregation system consists of a novel combination of methodologies that together provide high separation efficiency under the extreme conditions of chemical looping systems.

Experimental results obtained from this project have shown that separation of char from varying particle size distributions of oxygen carrier (ilmenite) are achievable under both ambient and elevated temperatures (300-400°C). Tests show that separation efficiency is directly impacted by the average particle size of the oxygen carrier relative to char. Results suggest that as oxygen carrier particles undergo attrition due to cycling in a chemical looping combustion system, a higher oxygen carrier recycle (split) is necessary in order to maintain high separation.

The technology and test methods developed have demonstrated the ability to improve carbon capture rates within chemical looping combustions systems and will continue to undergo development with the goal of lowering greenhouse gas emissions from fossil fuel combustion.

## CHAPTER I

### INTRODUCTION

Due to dependency on fossil fuels for energy production, the global atmospheric concentration of  $CO_2$  has increased strongly to about 397 ppm in 2015 [1]. Concentrations above 450 ppm are considered to lead to catastrophic climate change, which is only 15% over today's value. A reduction in emissions of greenhouse gases, particularly  $CO_2$ , is necessary.

Several strategies are being considered and deployed to reduce  $CO_2$  emissions, including reducing energy consumption, increasing energy efficiency, switching to less carbon-intensive fuels (natural gas instead of coal), increasing renewable energy sources, and use of nuclear energy. However, no single technology option is likely to provide a majority of emissions reduction. In this context,  $CO_2$  capture and storage (CCS) appears to be a necessary and additional option. According to some recent studies [2,3], CCS could account for about 20 percent of the total  $CO_2$  emission reductions needed to stabilize climate change impacts.

#### Chemical Looping Combustion

Chemical Looping Combustion (CLC) has emerged as an attractive alternative for  $CO_2$  capture, where a near-pure  $CO_2$  stream is produced from fossil fuel combustion without the use of oxygen obtained from air separation. In this type of system, a solid carrier is used to bring oxygen to the fuel to convert it to a pure  $CO_2$  stream. The solid is then regenerated (oxidized)

separately using air. This technology is expected to be more cost-effective and energy efficient compared to oxygen separation from air by other processes.

Figure 1 presents a simplified schematic for the CLC process. The oxygen carrier (OC) is usually a solid, metal-based oxide ( $M_XO_Y$ ). In the fuel reactor, the OC material reacts with the introduced fuel to release oxygen and oxidize the fuel. In this manner, the products of fuel oxidation ( $CO_2$  and  $H_2O$ ) are kept separate from the rest of the flue gases/nitrogen, resulting in a concentrated  $CO_2$  stream. The fuel reactor typically operates at an elevated temperature (700-1000 °C). After reaction in the fuel reactor, the OC, now in its' reduced form ( $M_XO_{Y-1}$ ), is cycled to the air reactor (typically 800–1000°C) where it is oxidized. Heat is extracted from the gases leaving the fuel and air reactors to produce steam, drive a turbine, and generate power. The overall chemical reactions in the two reactors, shown for an iron oxide OC, can be expressed as:

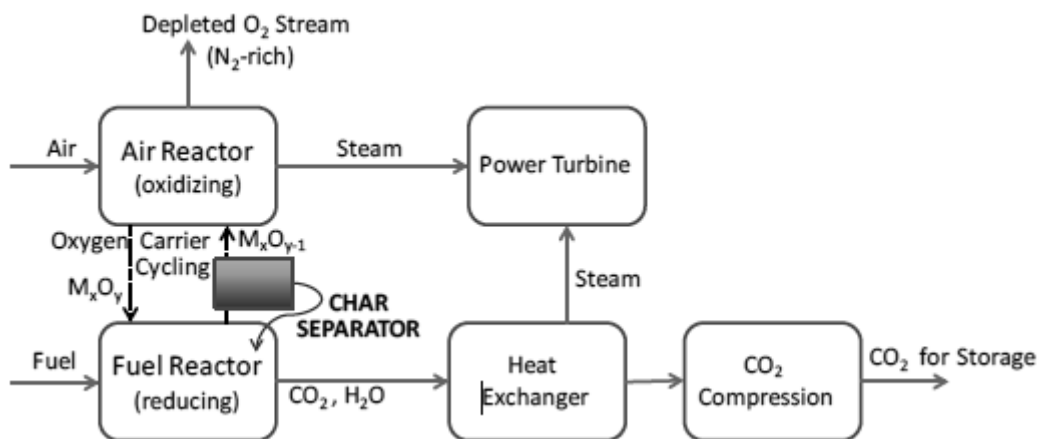
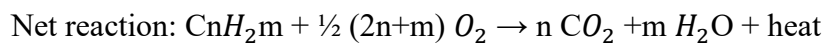
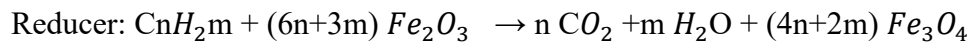
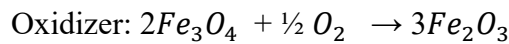


Figure 1. Process Schematic for Chemical Looping Combustion

## The Problem

When a solid fuel is used, only a portion of the fuel is converted in a single pass in the fuel reactor. This necessitates the need for segregation of the material leaving the fuel reactor into unconverted fuel (char) and OC, performed by a char separator. The separated char can be returned to the fuel reactor to increase its conversion.

If unconverted fuel is transferred to the air reactor, it would be combusted in air releasing its CO<sub>2</sub> with the N<sub>2</sub>-rich gases. Since the primary motivation of chemical looping technology is to achieve a high carbon capture rate (CCR), an efficient char separator is mandatory. The CCR is the percent of fuel carbon that is converted to CO<sub>2</sub> in the fuel reactor. The design and development of such a char separation device is the object of this research project.

## Oxygen Carriers (OC)

The oxygen carrier is the most important component of a CLC system. The role of an OC is to transfer O<sub>2</sub> between air and fuel efficiently. Suitable oxygen-carriers for solid fuels in the CLC process must have selectivity to form CO<sub>2</sub> and H<sub>2</sub>O, enough oxygen transport capacity, high reactivity, high mechanical strength, attrition resistance, and negligible agglomeration tendency. Besides these, the OC must also be abundantly available, environmentally benign and inexpensive. Each of the different types of oxygen carriers are discussed further below, with their particular suitability for use with solid fuels.

### *Copper-Based Materials*

Copper-based materials have shown to be very reactive, with full combustion of gasification products at a mass ratio of OC/solid fuel of only 10:1 at 850 °C [4]. Cu-based oxygen carriers are especially suited for a chemical looping with oxygen uncoupling (CLOU)

process, where oxygen is released from the carrier in the fuel reactor. Copper-oxygen carriers prepared by impregnation on SiO<sub>2</sub>, TiO<sub>2</sub>,  $\gamma$ -alumina or co-precipitation with alumina [5] have excellent chemical stability and mechanical strength after multi-cycle testing. Other supports have shown unacceptable levels of attrition. The main concern with Cu-based oxygen carriers is agglomeration due to melting. A content of less than 20% CuO was required to avoid agglomeration issues. Forero et al. [6] analyzed the behavior of a Cu-based oxygen-carrier with  $\gamma$ -Al<sub>2</sub>O<sub>3</sub>. Stable operation for more than 60 h was only feasible below 800 °C in the fuel reactor and 900 °C in the air reactor.

Adánez et al. [7] prepared stable bimetallic Cu-Ni/Al<sub>2</sub>O<sub>3</sub> particles and observed that the presence of NiO in the oxygen carrier stabilized the CuO phase. Long-term tests in a CLC unit under continuous operation showed high metal oxide utilization, and low and stable attrition rate after 67 h of operation at high temperature. This was the first time that a Cu-based oxygen-carrier, prepared by a commercial manufacturing method, exhibited good behavior at these temperatures.

The required inventory of Cu-oxygen carrier is significantly lower (120-200 kg/MWth) compared to other OCs (e.g. Fe-based OC-2000 kg/MWth). Even with lower inventory requirement, the significantly higher cost implies that it needs to have high particle lifetimes and excellent attrition resistance. Density of the Cu-based OC ranged from 3700-5400 kg/m<sup>3</sup>.

### *Iron-based Materials*

Iron-based materials represent an abundant, low cost, environmentally benign alternative for OC material, but have much lower reactivity and consequently a high OC to solid fuel ratio (50-100:1) which results in a low overall char content making separation a challenge. At Ohio State University [8], the iron-based OC developed incorporates inert support materials,



increasing the reactivity and recyclability. A 200-hour test performed in a 25 kWth chemical looping facility with lignite and sub-bituminous coal was presented by Bayham et al. [9], and showed minimal CH<sub>4</sub> /CO/H<sub>2</sub> slippage through the fuel reactor. Particle size of the oxygen carrier was around 1.5-5 mm, the fuel reactor was operated as a moving bed and the air reactor as a fluidized bed. Other researchers have used Fe-based carriers, including Leion et al [10]. An OC of 60 wt.% Fe<sub>2</sub>O<sub>3</sub> and MgAl<sub>2</sub>O<sub>4</sub> as inert was used with petroleum coke as the fuel. High reactivity was found with the gasification products (H<sub>2</sub> and CO) of coke with steam. Shen et al [11] used a biomass fuel in a continuous 10 kWth CLC system and accomplished a 30 h test. The fuel reactor temperature was varied between 740 and 920°C and CO<sub>2</sub> was used as a gasification medium. Low reactivity of the oxygen carrier was observed due to sintering.

The use of cheap natural minerals such as ilmenite (iron titanate) represents another promising OC candidate. Berguerand and Lyngfelt [12,13] operated a 10 kWth unit using coal and petroleum coke; combustion efficiencies of 85-95% were obtained. Thon et al. [14] used ilmenite in the size range of 100-400 microns. The solid fuel was lignite with 70 percent smaller than 150 microns. Activated ilmenite (after circulating in reactor system) was determined to have a density of about 3600 kg/m<sup>3</sup> [15]. Results also showed a low tendency for attrition and agglomeration for this material and its low market price makes it a promising option for use as an oxygen carrier.

#### *Calcium-based Materials*

General Electric (GE) Power (formerly Alstom) is developing a CLC process where CaSO<sub>4</sub> is used as oxygen-carrier for heat generation, syngas production or hydrogen generation [16]. Density of CaS is around 2600 kg/m<sup>3</sup>. The size of the OC used is comparable to bed ash from a circulating fluid bed combustor, with the coal being finer.

### *Manganese-based Materials*

Although a promising metal oxide, Mn-based oxygen carriers have not been widely tested so far. The disadvantage of manganese oxides is their incompatibility with common support materials like Al<sub>2</sub>O<sub>3</sub> and SiO<sub>2</sub>. Mn-based OC supported on ZrO<sub>2</sub> stabilized with MgO has shown good reactivity with syngas components [17], but lower reactivity has been found for CH<sub>4</sub> [18]. These particles have also been tested in a continuously operated 300Wth CLC unit [19]. Absence of agglomeration and low attrition rate were observed. Very high efficiencies (>99.9 %) were obtained at temperatures in the range 800-950 °C for syngas combustion.

Arjmand et al. [20] evaluated the CLC performance of various manganese ores with two fuels, petroleum coke and a wood char. The particle size of the OC was 150-350 microns and activated densities ranged from 2200-3600 kg/m<sup>3</sup>. Fuel particles used were 180-250 microns, similar in size to the OC.

#### *Attrition and its impacts on char/oxygen carrier separation*

The attrition behavior of OCs is an important characteristic for char/ash separation as the particle size distribution of the fresh OC is only partly relevant for an operating system. Because of attrition, the size of the circulating OC will be finer than the fresh material. This reduces differences in the terminal velocity values for the char and the OC, making efficient separation more difficult. All OCs have a limited lifetime, either because of reactivity loss, or due to attrition processes that elutriate the OC particles out of the system.

In summary, particle densities of OC vary from about 2200 to 5000 kg/m<sup>3</sup>. On the other hand, char densities vary from 500-800 kg/m<sup>3</sup>. The density ratio ( $\rho_{OC}/\rho_{char}$ ) varies from 3-10. With an appropriate choice of the size ratio of the OC to coal, a terminal velocity difference-based method may be used as a partial basis for separation of the char from the OC. However,

overlapping terminal velocities for a part of the OC material (small size) and char (large size) necessitates that alternate characteristics be used for good separation.

### Current Char/OC Segregation Methods

Due to its importance to CLC technology, there has been significant research into development of carbon separation methods for CLC in recent years. Several methods can be used to separate the char, ash, and OC particles from each other based on differences in size, density, terminal velocity, magnetic properties, and triboelectric properties. However, the high temperature condition (800-1000 °C) precludes most methods. Based on a review of various separation methods, it was concluded that those based on size/density are the most promising. The following sections outline some of the recent work.

Sun et al (2015) [21] developed a 70 kW CLC cold flow model with a carbon stripper that consisted of a 4-chamber fluidized bed in which the bottom of the bed was operated in a turbulent fluidization regime and the top of the bed, due to its decreasing cross-section, acted as an elutriating bed for the small/light particles that escaped to the surface of the lower turbulent bed. A simulated OC/carbon mixture was used made up of ilmenite particles and Plexiglas beads representing the carbon particles, with the ilmenite having a slightly larger size distribution. A maximum of only 60% separation of the Plexiglas beads was achieved.

Sun et al (2016) [22] developed a cold flow riser-based carbon stripper that used a mixture of ilmenite and plastic beads to simulate the OC/char mixture, both with a relatively narrow size distribution and the plastic beads being slightly smaller than the ilmenite. Results indicated good plastic beads separation (>90%) when operating at sufficiently high velocity, but at the expense of significant elutriation of the ilmenite with the plastic beads.

In their 1 MWth pilot plant, Ströhle et al (2015) [23] operated a carbon separation system that consisted of two cyclones in series and a fluidized bed carbon stripper. The larger/heavier particles were separated first in a low-efficiency cyclone, which were then routed to an elutriation-based fluid bed to separate the carbon from the OC. The non-elutriated OC-rich fraction was routed to the air reactor, with the elutriated carbon-rich fraction returned to the fuel reactor. The particles bypassing the low-efficiency cyclone were routed to a high-efficiency cyclone where the smaller/lighter particles were separated and returned to the fuel reactor. Due to issues with using pulverized coal as the fuel, poor carbon burnout was achieved in the fuel reactor, and a large quantity of the unburned carbon bypassed the high-efficiency cyclone.

Abad et al (2015) [24] developed the conceptual design of a 100 MWth CLC system, in which an elutriation-based carbon stripper was used. According to their models, very high carbon separation efficiency could be achieved (~99%) when using small fuel particles (Average particle size = 47 $\mu$ m) under the appropriate fluidization velocity.

Markstrom et al (2013) [25] of Chalmers University, Sweden used a multi-section bubbling bed with a tortuous path to prevent short-circuiting. The particle size of the coal used was finer than the OC and they achieved good carbon separation, recycle, and high (>90%) CO<sub>2</sub> capture efficiency. However, given the short-term test periods used, they did not account for the expected size reduction of circulating OC, which would reduce the terminal velocity differences between the char and the OC and lower separation efficiencies.

The above examples are just a few of the current efforts related to carbon separation devices for CLC. In most cases, a terminal velocity-based entrainment method is employed, which can be aided by the use of cyclones. However, in the above examples realistic mixtures of OC/char were not used due either to simulated mixtures or relatively short operating test periods.

In an actual system, due to OC attrition, there is likely to be a very broad size distribution of the OC. Additionally, the density of the carbon particles cannot be assumed to be that of pure carbon due to association with fuel ash, as well as agglomeration/sintering mechanisms that result in difficulty in removing the carbon/ash from the OC. There is likely to be a broad distribution of both the content of carbon within and the density of the carbon-containing particles in the solids mixture. These challenges result in a significant overlap of the entrainment parameters of the OC/char, making it unlikely for an elutriation-only system to be successful in achieving a high carbon capture rate (CCR) without significant recycle burden of OC to the fuel reactor. Rather, it will likely be necessary to use a multi-step approach with methods specifically targeting ranges of particle size and density. Our proposed approach addresses the shortcomings of current work in such a manner.

### The Solution

Figure 2 displays a schematic of a particle char separator (PCS) system, which is the optimum configuration as identified from the proof of concept phase of the project for a calcium-based OC. To separate the carbon from the OC, the distributed mixture of solids leaving the fuel reactor in the CLC system is sent to the PCS. The PCS comprises two main components which are discussed below.

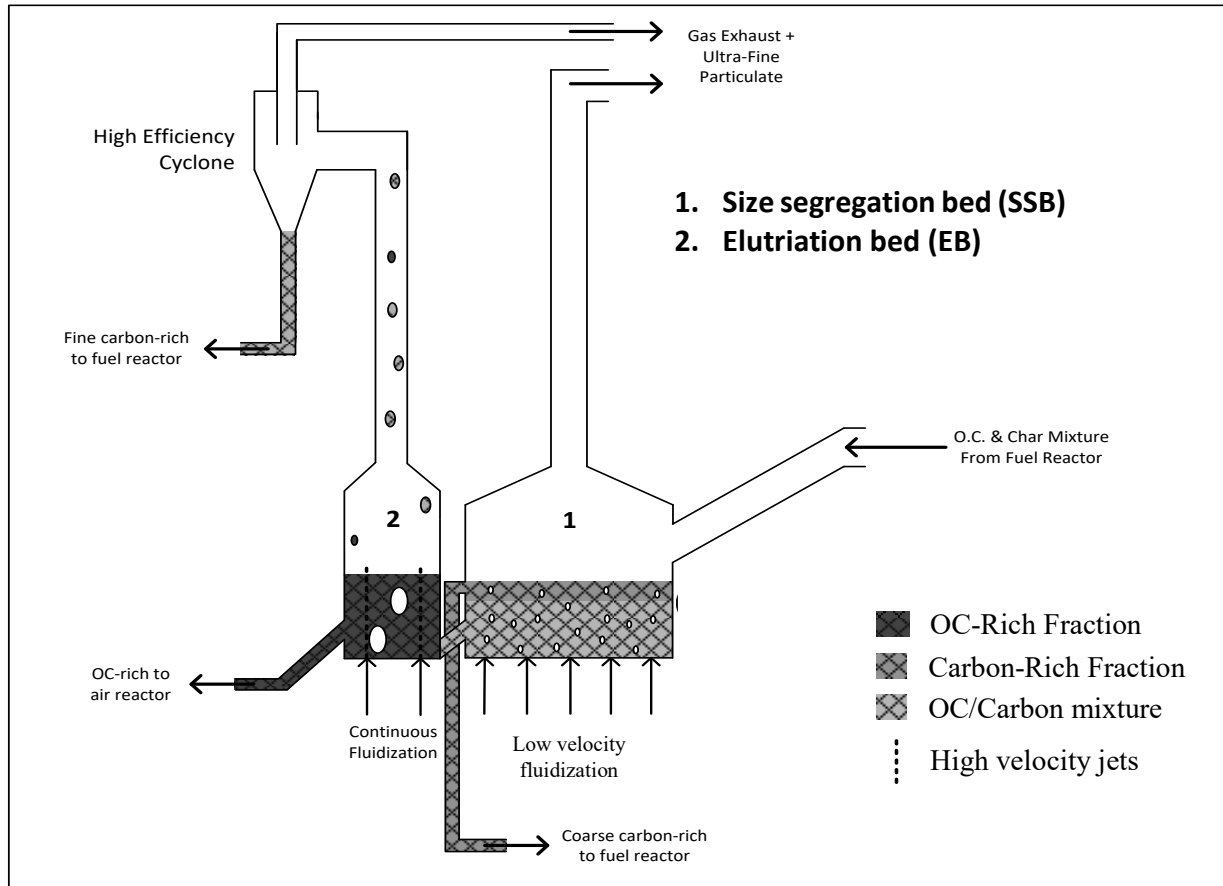


Figure 2. Char Separation System

*Size segregation bed (SSB)*

Through a combination of hydrodynamic fluidization regimes, the coarse carbon-rich particles (lower density than OC) are preferentially segregated to the top of the fluidized bed. Details regarding the fluidization regimes are proprietary and therefore cannot be discussed. The carbon-rich top layer is removed from the SSB by spilling over a weir and recirculated to the fuel reactor while the carbon-depleted bottom layer is sent to the next stage of the PCS system.

*Elutriation bed (EB)*

With the largest carbon-rich particles removed in the SSB, the EB is run at a relatively moderate velocity to elutriate the remaining fine-sized carbon-rich particles. A high efficiency cyclone captures the elutriated carbon-rich particles, which are recirculated to the fuel reactor.

The non-elutriated bottom layer, consisting of the carbon-depleted OC is sent to the air reactor of the chemical looping combustion (CLC) system for regeneration.

### *Project Objective*

The objective of this project was to design, fabricate, and test a hot flow char separation system utilizing past proof-of-concept work in order to identify optimum operating conditions. This thesis consists of all design processes that lead to the final product, as well as any changes/improvements that were made during the initial testing period. Relevant calculations are shown to support design. To ensure the best separation was achieved, several operating conditions were varied and documented. For each variable changed, multiple test runs were made to demonstrate repeatability. Results from each variation were analyzed to determine the optimum conditions. Process conditions that were varied include the combinations of gas velocities of the size segregation bed, as well as the gas velocity of the elutriation bed. Results reveal what operating conditions are necessary to achieve the best separation of solids based on size/density.

### *Approach*

It is critical that the char entering the air reactor is minimized in order to have a high CCR. With this in mind, the configuration of the particle char separation (PCS) system is set up to maximize purity of the OC going to the air reactor, even at the expense of a slightly larger OC recirculation load (split) to the fuel reactor. Discussions with GE Power suggests that 20% recycle can easily be tolerated. Given this, combined with the results of the proof of concept phase, it is expected to be able to achieve greater than 80 % separation of the carbon leaving the fuel reactor.

The PCS system is a multi-step approach with unit operations that target specific ranges of particle size and density to mitigate the challenge of a large overlap in the entrainment parameters of the OC and carbon-rich particles. Rather than undergoing a single “treatment,” the OC undergoes two steps to ensure maximum removal of the carbon. The PCS approach offers a high degree of flexibility in terms of both configuration and operating parameters to optimize operation based on the properties of the material being segregated and overall CLC process requirements.



## CHAPTER II

### PROOF OF CONCEPT

The first step in this work was the development of a two-step separation methodology for char/OC separation. The proof-of-concept of the char-OC separation for Chemical Looping Combustion (CLC) systems was demonstrated through laboratory-scale evaluation of the multi-step separation process with cold flow systems. The operating window and carbon separation performance were determined in a previous project prior to this research. The project identified the optimum Particle Char Separator (PCS) configuration for the oxygen carrier (OC)-char mixture that was used during the tests. It also revealed enhancements to the PCS design and configuration which would be expected to improve performance and system operability significantly. Testing showed that char separation from the OC is feasible with key accomplishments summarized below:

- Carbon was successfully separated from a synthetic test material of glass beads/activated carbon during concept verification experiments.
- An oxygen carrier-char material obtained from the GE Power pilot test unit with a carbon content of 1.4% was tested in the laboratory-scale PCS test systems. A very broad size distribution of the OC and carbon-rich particles represented a realistic and very challenging material for separation testing.

- Testing on the first unit – Size Separation Bed (SSB) showed 25% to 30% of the carbon was separated into 10% of the total material, for an enrichment factor of 2.5. Significantly better separation was achieved in the coarse particles.
- Testing on the second unit – Elutriation Bed (EB) – showed approximately 43% of the carbon was separated with 8% of the material, for an enrichment factor of approximately 5 to 6. Significantly better separation was achieved in the fine particles.
- When combining the performance of the SSB and EB based on “coarse” and “fine” size fractions, the results were 55% and 70% carbon separation in 18% and 29% of starting material, respectively.
- Proof of concept testing identified the key operating conditions and factors governing separation efficiency for the SSB and EB.

It was found that the performance of the EB and SSB systems depends on the size distribution of the OC being separated and the distribution, size and association (i.e. discrete, OC or fuel ash) of carbon-rich particles in said material. Based on the results of the proof of concept, an ideal PCS configuration for the GE Power OC material will separate the coarse carbon particles first in the SSB, allowing the subsequent EB unit to be operated at a relatively low velocity, while targeting the fine carbon and avoiding excessive OC entrainment. The success of this research justified expanding the PCS proof-of-concept testing to operation at relevant CLC temperatures (~800°C) and understanding the impacts of a reducing fluidizing atmosphere (e.g. steam) and gas generation due to reactions on the separation method and efficiency.

## CHAPTER III

### DESIGN AND CONSTRUCTION

Prior to beginning construction of the hot flow system, a review of the design of the bench scale PCS system was necessary to finalize the specifications for the hot flow system. One area that needed review was controlling of the solid flow between beds. Initially it was planned to use screw feeders to transport the material between process components in the PCS. However, scale-up concerns related to the use of a screw feeder in a commercial system resulted in the designing of loop seals as a means to transport solids between the different beds.

The other area of the design that needed to be revisited was the final specifications such as the dimensions, operating conditions (flow rate), and system control of the SSB and EB. In order to address these concerns, cold flow units were constructed for the SSB and EB. A procured oxygen carrier and simulated char substitute were then tested on the cold flow unit. Results from the cold flow testing were used to finalize the hot flow design. The testing and results obtained from the cold flow units are discussed below.

#### Preparation of Test Materials

Two particle size distributions (PSD's) of fresh ilmenite were obtained from GE Power (formerly Alstom) following preliminary discussions on what oxygen carrier (OC) to test on the PCS system. The two batches of ilmenite consisted of a coarse and a fine PSD with average particle sizes of 230  $\mu\text{m}$  and 94  $\mu\text{m}$ , respectively. Ilmenite is a high density oxygen carrier that occurs naturally in its reduced form ( $\text{FeTiO}_3$ ) and is oxidized at high temperatures to

pseudobrookite ( $\text{Fe}_2\text{TiO}_5$ ) and rutile ( $\text{TiO}_2$ ) [26]. It has also been tested significantly and is considered a promising OC material [27].

Recent work done on another SBIR/STTR project – DE-SC0011984 – shows that fresh ilmenite, when subjected to several oxidation-reduction cycles, undergoes physical changes affecting particle density (porosity development) and size (fragmentation and attrition). Table 1 illustrates the change in bulk density of ilmenite after an oxidation-reduction (redox) cycling for 5000 minutes (approximately 400 cycles). The bulk density of “cycled” or “in-process” ilmenite is 40 percent lower than the fresh material. The corresponding true particle densities are approximately twice the values (i.e.  $\sim 2600 \text{ kg/m}^3$  for the cycled ilmenite material).

Table 1. Change in bulk density for an ilmenite sample cycled for 5000 min

Size Range ( $\mu\text{m}$ )	Fresh Ilmenite	Cycled Material (5000 min)
	Average Density (S.G.)	Average Density (S.G.)
840-500	2.1	1.3
150-105	2.1	1.3
105-75	2.1	1.3
<75	2.0	1.1

Table 2 shows the size distribution of the fresh ilmenite obtained from GE Power. Figure 3 shows the change in size distributions of the cycled ilmenite as a function of the number of cyclic operations. The data shows that when the larger size particles in the oxygen carrier inventory are subjected to cyclic oxidation and reduction in the chemical looping combustion process they undergo fragmentation and attrition. As a result, smaller size oxygen carrier particles (e.g. less than 53 microns in Figure 3) are created. These expected changes are important factors in the range of oxygen carrier properties that must be considered in the separation process.

Table 2. Ilmenite particle size distributions

Size ( $\mu\text{m}$ )	Coarse OC Distribution %	Fine OC Distribution %
>300	3	0
300-150	95	2
150-105	2	21
105-75	0	70
75 - 53	0	6
< 53	0	0

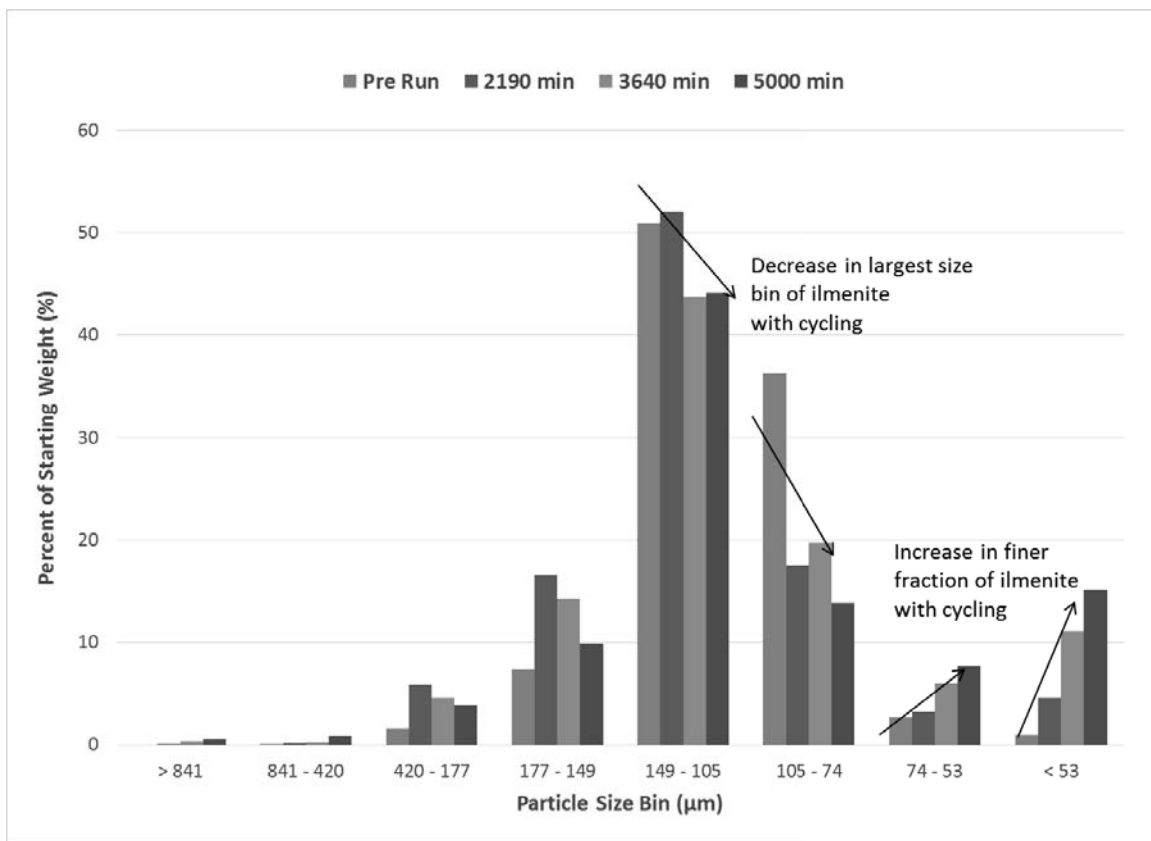


Figure 3. Change in ilmenite size distribution after 5000 min of redox cycling

Activated carbon (AC) and char were used to simulate the OC/char mix for the carbonaceous char component for the cold flow testing. Coal char was produced by pyrolyzing a Powder River Basin (PRB) sub-bituminous coal. Both materials were prepared to a size distribution similar to that observed for unburnt char in GE Power's pilot Chemical Looping Combustion (CLC) facility. The size distributions for the coarse and fine batches of ilmenite and

activated carbon can be seen in Figures 4 and 5, respectively. In order to evaluate the performance of the cold flow unit, the total carbon content of the AC and char was determined and results are presented in Table 3.

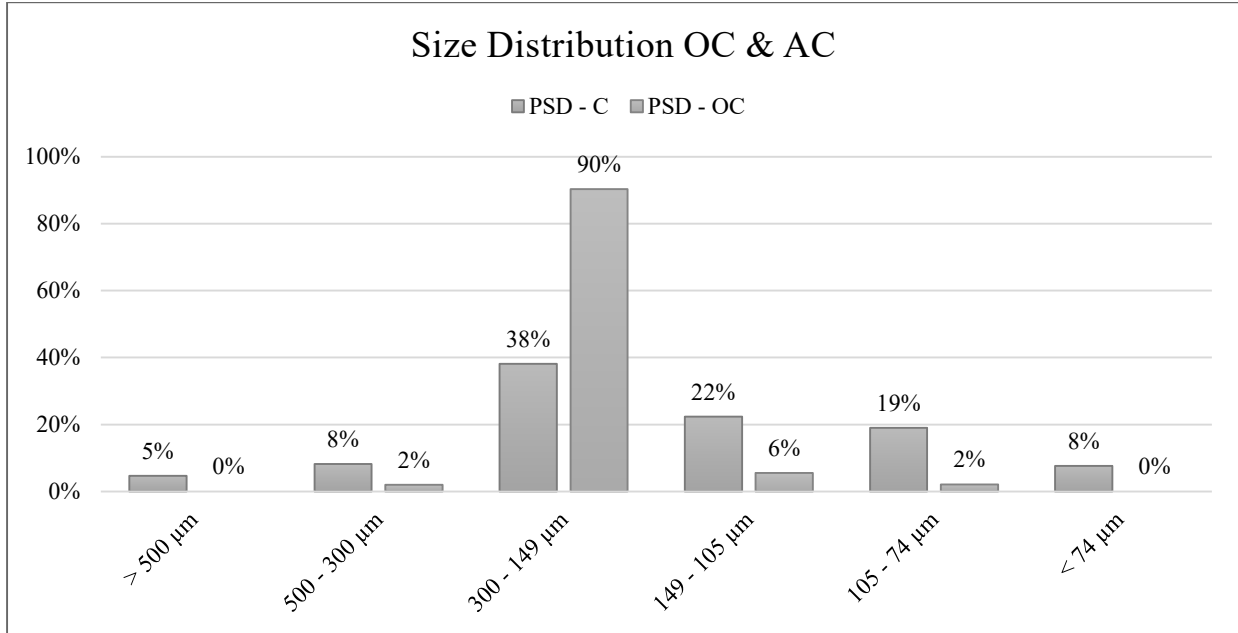


Figure 4. PSD of coarse OC and AC

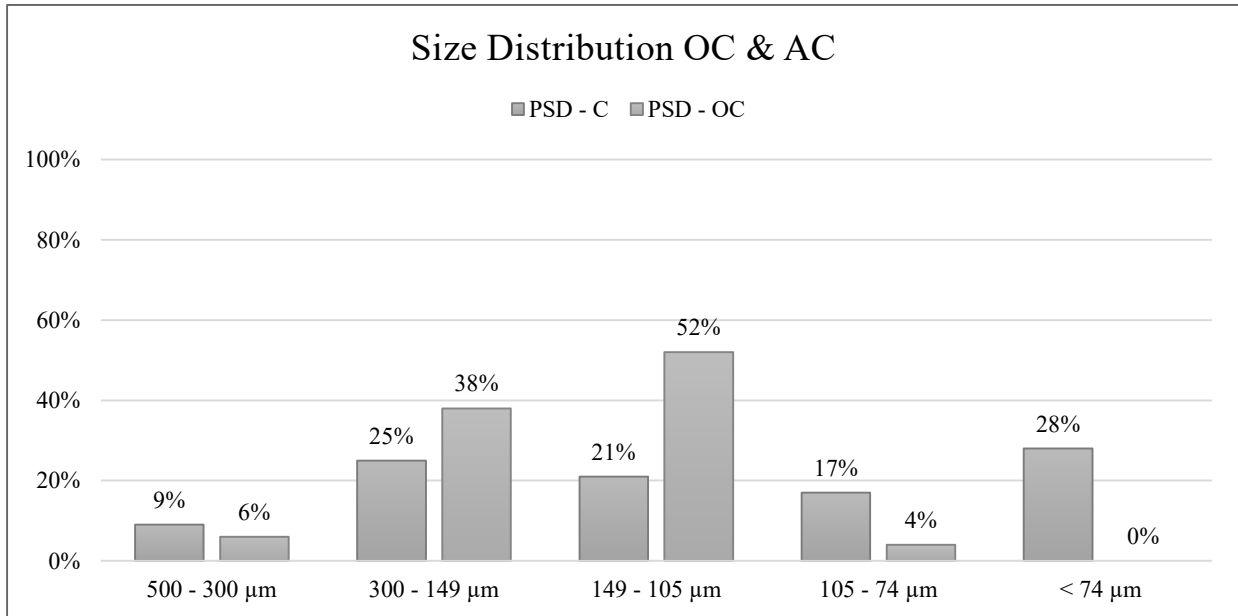


Figure 5. PSD of fine OC and AC

Table 3. Carbon content of AC and char for different size bins

Size ( $\mu\text{m}$ )	Carbon Content	
	AC	Char
> 300	84%	67%
300 - 150	83%	64%
150 - 105	82%	66%
< 105	80%	67%
<b>Average</b>	<b>82%</b>	<b>66%</b>

### Loop Seal Design

In the initial test equipment design, material flow between process components was to be controlled using high temperature screw feeders between each unit. However, due to the high cost of custom high temperature screw feeders, it was required that an alternative solution be developed. A loop seal was designed based on literature [28] and modified to operate similar to an L-valve by providing fluidizing air on the feed leg only. A proof-of-concept loop seal was constructed out of 1-inch-thick acrylic sheets and tested using the procured ilmenite. Flow to the loop seal was controlled using a mass flow controller and the solids feed rate of the loop seal was determined for varying flow rates. Figure 6 shows the calibration results using the coarse ilmenite which demonstrate that it was possible to vary the material transfer rate in a predictable manner by varying the fluidizing air flow to the loop seal.

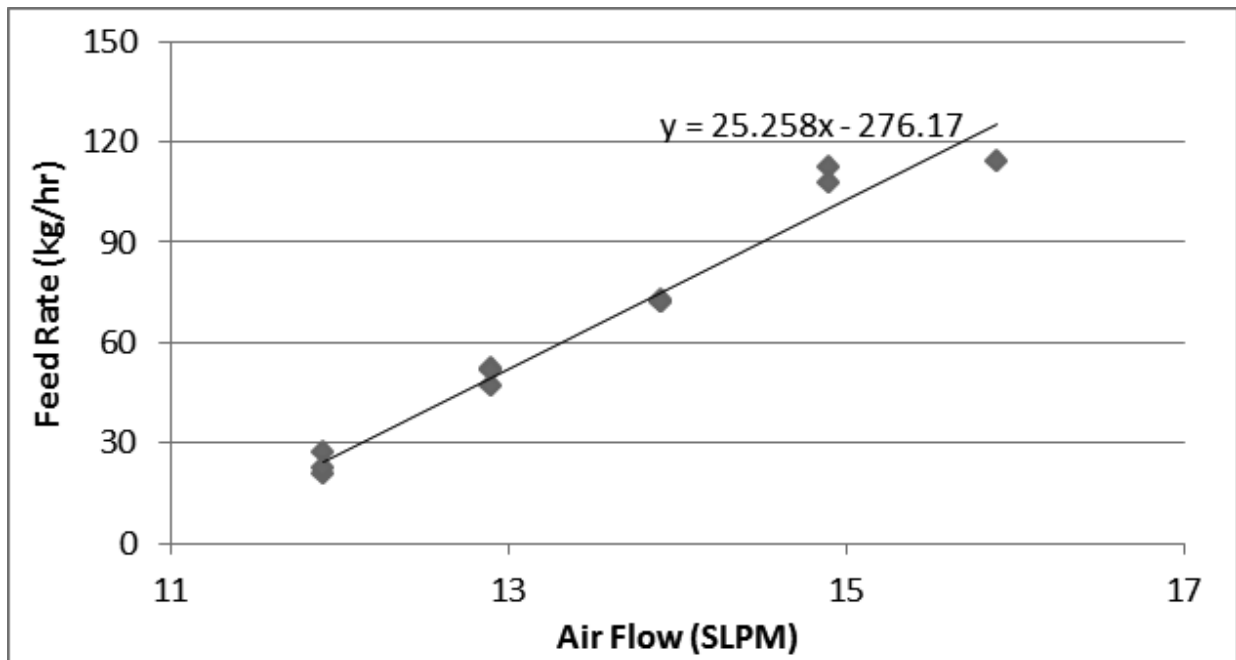


Figure 6. Cold flow loop seal calibration for coarse ilmenite

Following successful operation of the temporary loop seal, two hot flow loop seals were constructed out of stainless steel. Figure 7 shows an image of one of the loop seals and a cross-section schematic of the design. The loop seals were then installed on the cold flow units of the EB and SSB for testing.



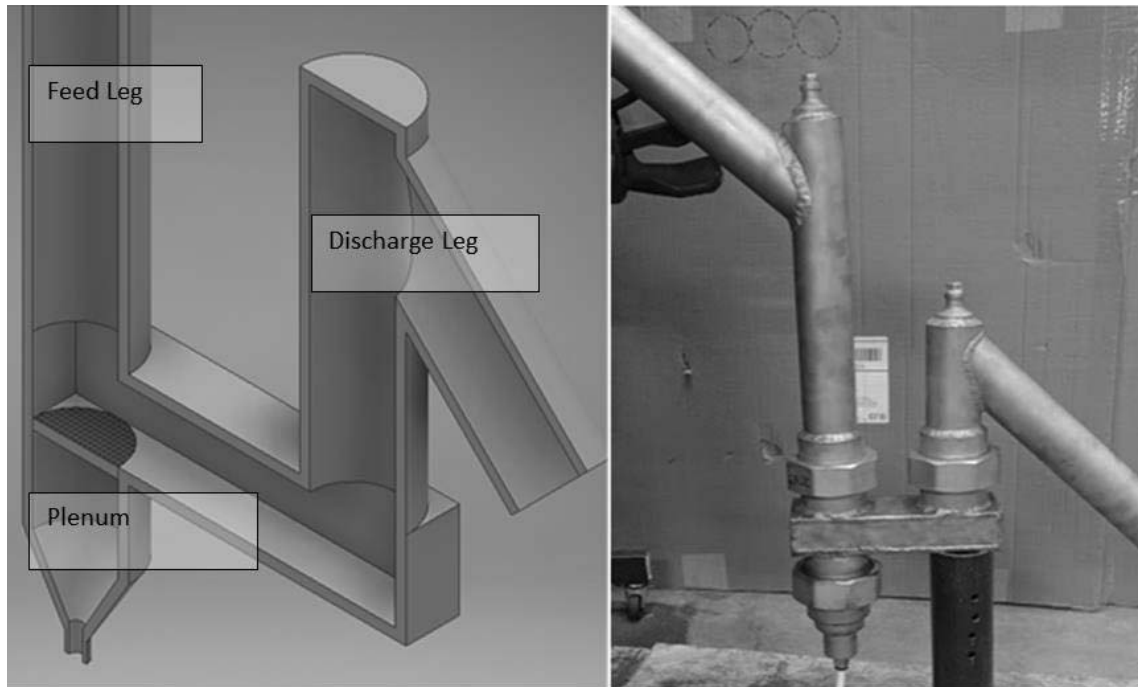


Figure 7. 3D cross-section of the original loop seal design (left) and an image of the constructed loop seal (right)

During operation, it was observed that material flow rates were a function of one additional parameter besides the fluidizing air flow – the particle size distribution (PSD) of the feed material. Material that contained smaller particle sizes required less air flow to obtain similar solid feed rates to that of the large particle sizes. Figure 8 shows calibration of the loop seal using fine ilmenite. It can be seen that to obtain a material feed rate of 50 kg/hr a gas flow rate of 2.8 slpm is required, whereas using the coarse ilmenite a gas flow rate of 12.9 slpm is required.

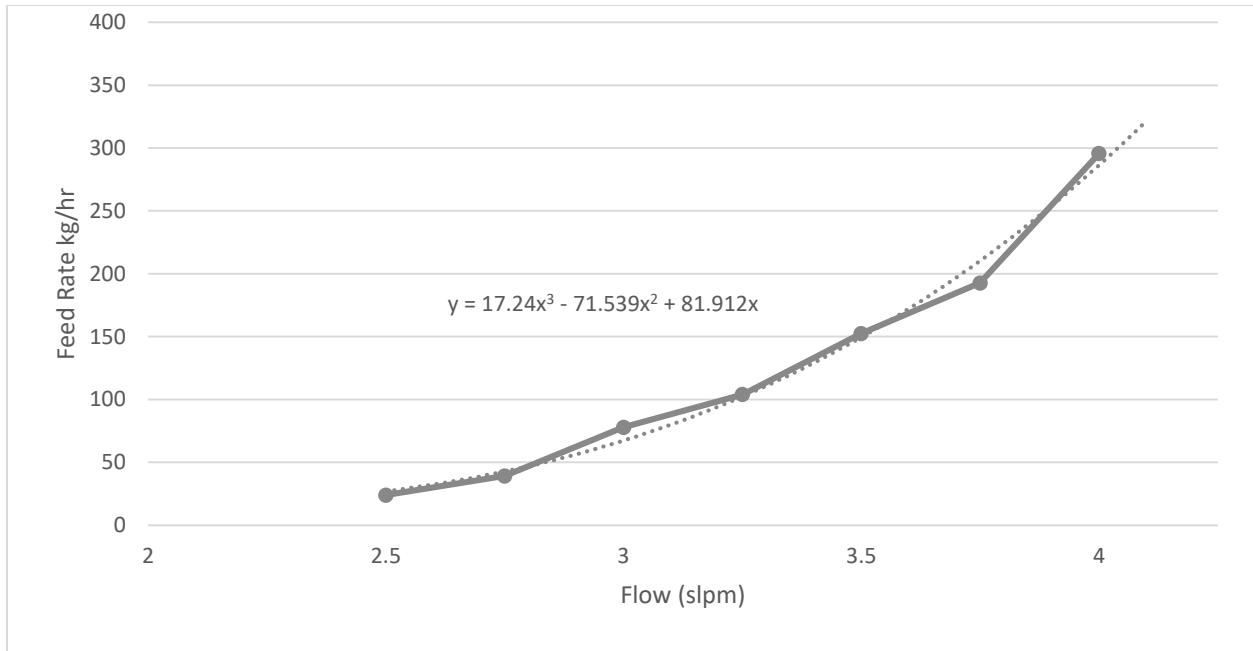


Figure 8. Loop seal calibration using fine ilmenite

It was later discovered during hot flow testing that these lower flow rates make consistent operation of the loops seals difficult. This is due to the high sensitivity of the loop seal design to air flow as well as the fact that the mass flow controllers (calibrated for nitrogen/carbon dioxide) were sized to be able to achieve high flow rates for the coarse ilmenite, resulting in lower resolution at low gas flow rates. Appropriately sized mass flow controllers would help resolve this problem, however, a re-design of the loop seal was found to be a more cost effective solution. Figure 9 shows three new loop seal configurations that were investigated. The new loop seal design consisted of a plenum with a divider located in the middle to allow for different configurations (A, B, and C) to be tested. Configuration “A” provided gas to both plenums equally, configuration “B” provided gas to the left plenum only, and configuration “C” provided gas to the right plenum as well as aeration gas on the inlet leg to allow for better material flow. The new design utilized quarter inch gas inlets and a 325 mesh screen as the distributor plate to prevent material from falling into the plenum.

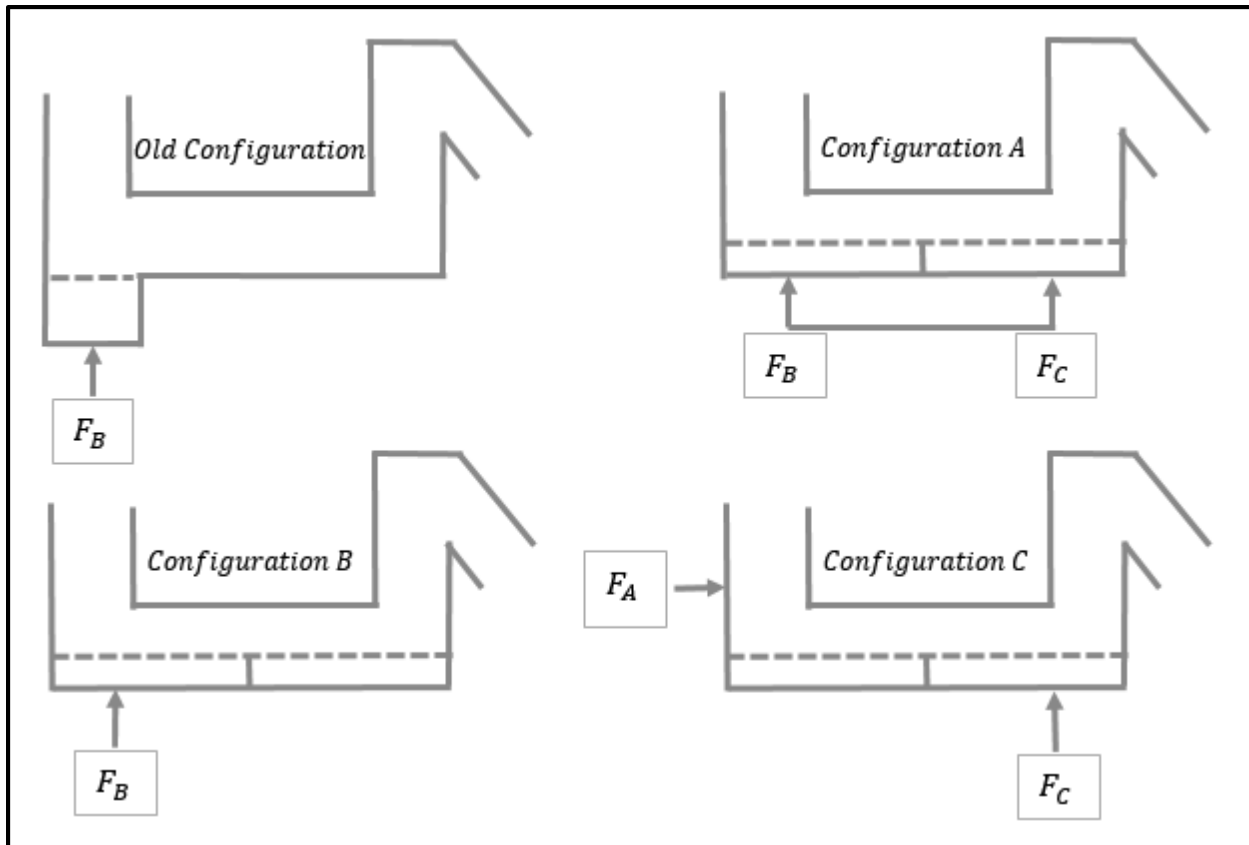


Figure 9. New loop seal configurations to be tested

Results from testing of the new loop seal designs can be seen in Figure 10. These results show that “configuration A” requires the highest gas flow rates for the desired material throughput (50 kg/hr). It can also be seen that “configurations A’s” feed rate stays linear the longest, making operation more predictable and consistent than other configurations. Using this data, the resolution for each configuration can also be found. Figure 11 shows the average percent change with 1 slpm increase in flow (sensitivity). It can be seen that “configuration A” has the lowest percent change (lowest sensitivity). These tests clearly demonstrated that “configuration A” of the new loop seal design would be easiest to control at the desired material feed rates. This new loop seal design was later implemented into the hot flow design.

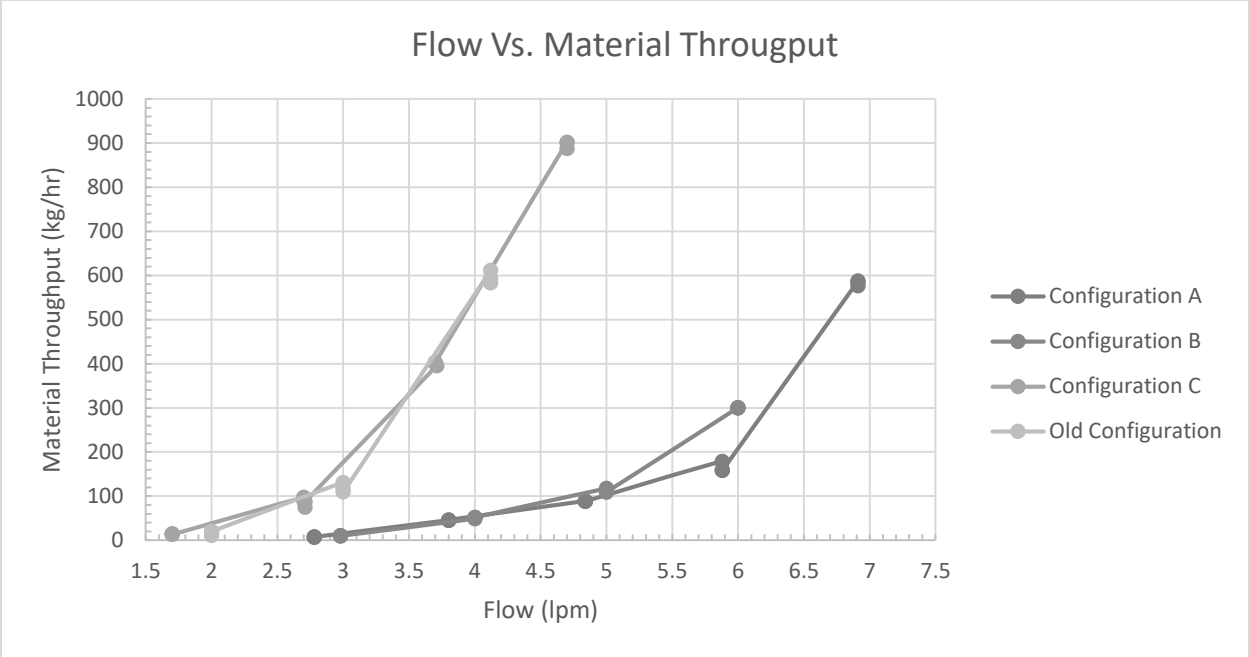


Figure 10. New loop seal design testing

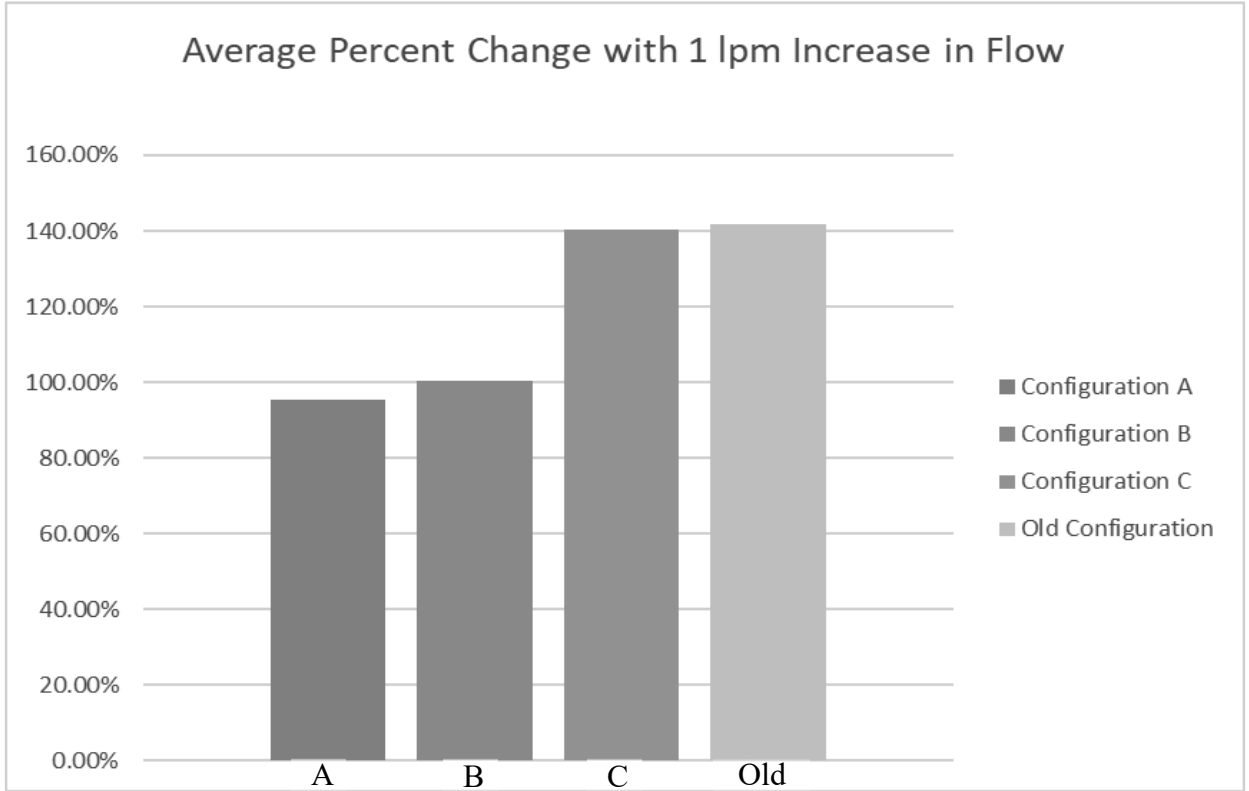


Figure 11. Comparison of new loop seal’s sensitivity to gas flow

During operation of the hot flow unit, additional parameters (discussed later) such as monitoring bed inventory will have to be used in addition to calibrated feed rates of the loop

seals. Nevertheless, the trend of increasing feed rate with increasing fluidizing flow was preserved and can still be used as a control mechanism. During hot flow testing, heat tapes rated to temperatures up to 760°C for continuous operation were used to heat the loop seals. Without the ability to maintain temperature between beds, the gas density would change as temperature decreases resulting in a change of material feed rates through the loop seals which would necessitate re-calibration.

### Design and Construction of the Feed Bed

The particle char separator (PCS) testing unit comprises four primary components, the OC/Char feed bed, the SSB and EB, and loop seals in-between. A PVC pipe was purchased and modified to serve as the feed bed for cold flow tests. The sizing of the cold flow bed was the same as for the hot flow. The hot flow feed bed was designed to hold a capacity of 100 kg of material heated to the desired temperature of approximately 800°C. It was constructed using Schedule 40 stainless steel due to the high resistance to corrosion and high temperatures. A grid plate made out of 325 mesh screen sandwiched between two perforated plates (quarter inch holes) for structural support was implemented for the purpose of providing nitrogen gas flow (less than minimum fluidization velocity) to the bed. The flow of nitrogen is necessary to ensure an inert environment is maintained to prevent burning of the char as well as to prevent agglomeration of the ilmenite particles at 800 °C. Low gas flow rates were necessary to prevent any pre-separation of particles that may occur at minimum fluidization velocity. Table 4 summarizes the specifications for the feed bed and Figure 12 shows images of the cold flow feed bed system and hot flow system under construction.

Table 4. Feed bed specification

Feed Bed Specifications		
Height	1.3 m	4.3 ft.
Internal Dimensions	0.2 m	0.67 ft.
Ilmenite Capacity	100 kg	220 lb.
Ilmenite Heat Capacity	0.9 kJ/(kg . K)	0.22 BTU/(lb.°F)
Ilmenite Packing Density	2400 kg/m <sup>3</sup>	500 lb./ft <sup>3</sup>
Heat Duty	14 kW	48000 Btu/hr.
Operating Temperature	800°C	1472°F
Temperature Ramp	2 – 3 hours	

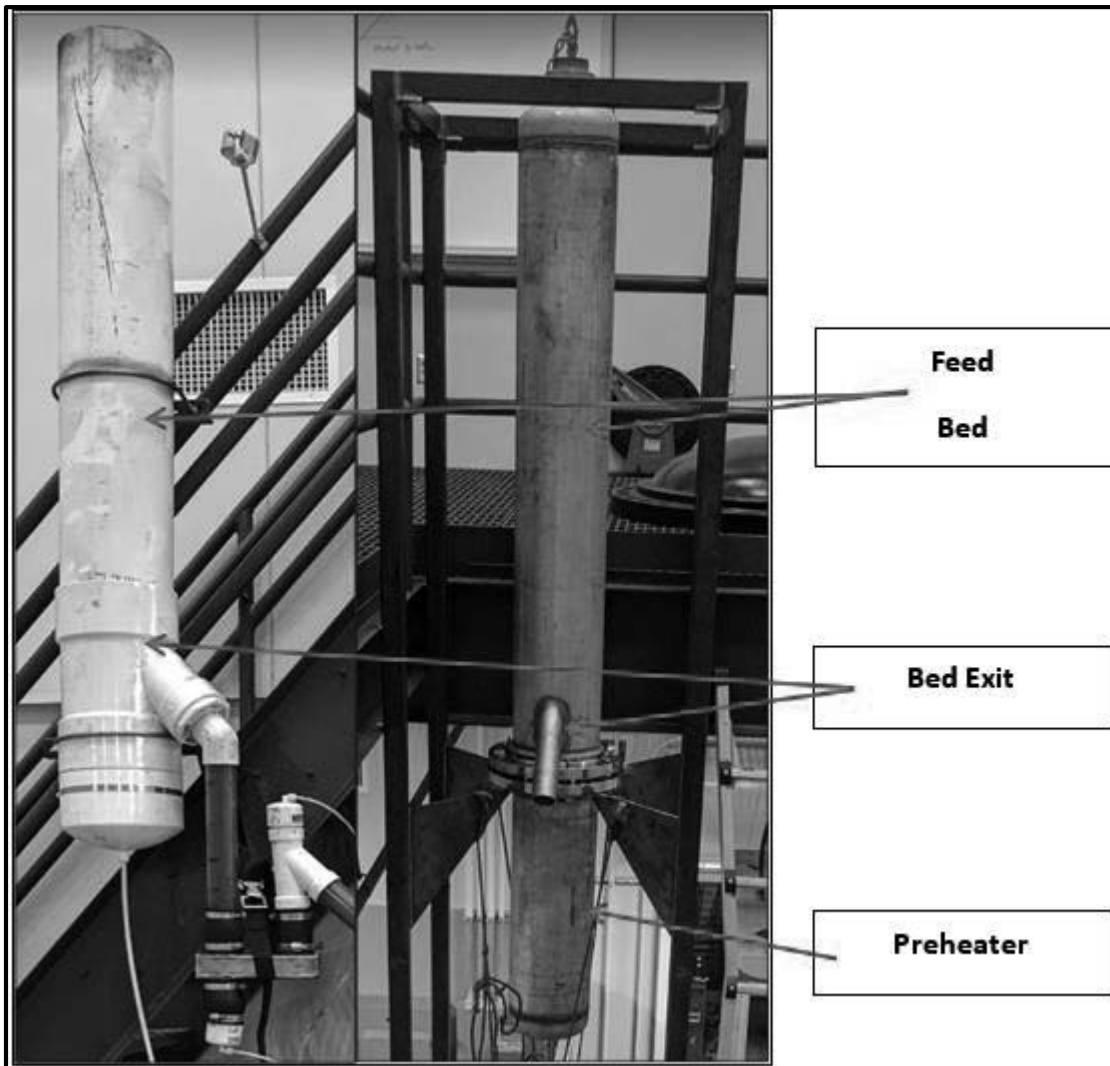
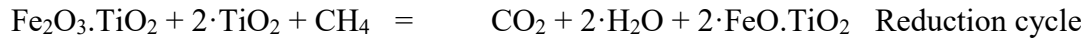
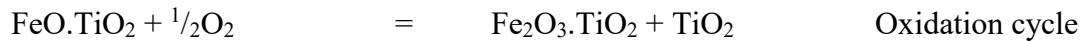


Figure 12. Cold flow feed bed (left) and hot flow feed bed system under construction (right)

Construction of the hot flow system feed bed includes four external 3.5 kW heaters for heating the OC and two external 3.5 kW for pre-heating the fluidizing gases. Thermocouples are installed in three zones (top, middle and bottom) of the bed to monitor the temperature. Two mass flow controllers (MFC) for nitrogen/air and methane are used to supply the inert/oxidizing and reducing gas respectively, during operation.

To account for the expected change in porosity during redox cycling of ilmenite, the feed bed will be used to “condition” the “fresh” ilmenite by subjecting to several redox cycles. The oxidation and reduction (with methane) equations of ilmenite are:



Based on the reduction and oxidation equations for ilmenite and methane and assuming only 50% of the 100 kg of ilmenite is reduced during each cycle (to ensure the methane is completely consumed), approximately 840 liters of methane will be needed per reduction cycle. At a planned methane feed rate of approximately 12 liters/min and a purge cycle of 20 minutes, it will take 80 min per reduction cycle. Assuming oxidation will be completed in 1 hour using house air, a complete cycle of the material will take approximately 3 hours. Based on other research, 15 cycles are considered sufficient to transform the ilmenite to its more porous form.

### Design and Construction of the Elutriation Bed

A cold flow elutriation bed (EB) unit was constructed first with the goal to verify/replicate the results obtained during the proof-of-concept testing and to confirm that a bed velocity of 30 cm/s was sufficient to elutriate the target material. Figure 13 is an image showing the cold flow unit and the construction of the hot flow unit.



Figure 13. Cold flow EB unit (left) and hot flow EB unit with air preheater (right)

The unit was constructed from an 8 cm (3 inch) schedule 40 PVC clear pipe with 60 cm between feed and exit locations (maximum bed height) and a free board above the inlet point of 25 cm. A 325 mesh screen was used as the grid plate and a fabric filter was installed on the exit to capture elutriates. Two of the constructed loop seals were used to control feed into and out of the unit. Fluidization was achieved using compressed air and a rotameter for control of gases.

The EB feed pressure during testing was monitored and a proportional response to material bed height was observed on the pressure sensors as shown in Figure 14. Bed pressure is seen to increase, stay stable, then decrease as the bed fills up, maintains stable, then decreases; respectively. This observation is important as it can be combined with cold flow calibration of the loop seals to maintain bed inventory during hot operation and estimate system feed rates.



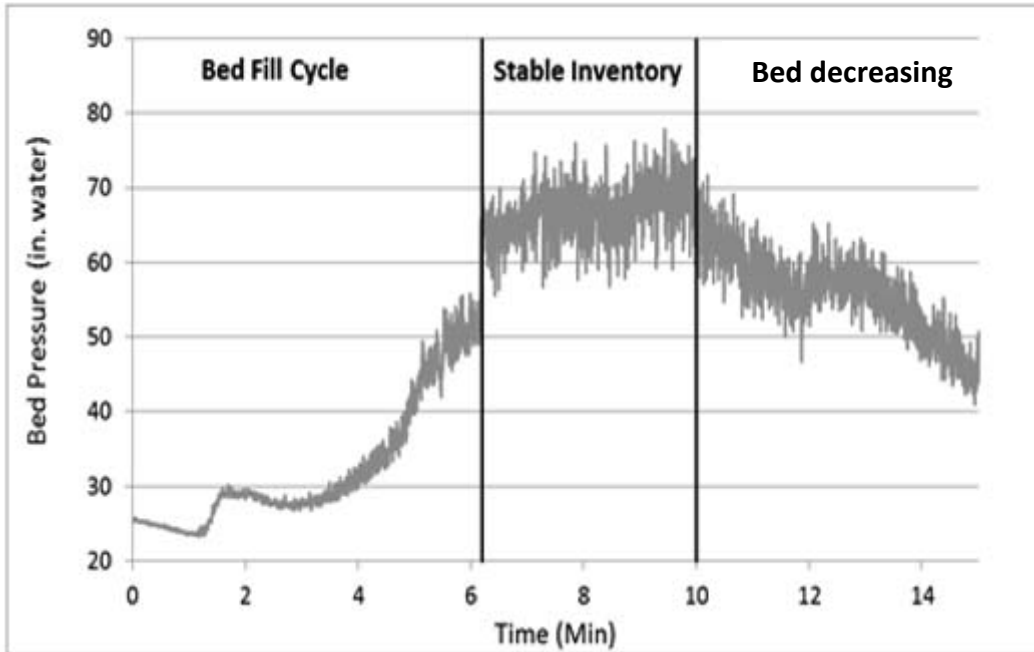


Figure 14. Bed pressure response as material is fed and removed from the bed

The final design specifications, gas velocity, and fluidization flow for cold and hot flow operation obtained for the EB are summarized in Table 5. The results obtained are for room temperatures and have been corrected for hot operating temperatures of 800°C at which gas volume and viscosity changes are significant. For gas volume, a temperature correction from 25°C to 800°C implies a decrease by a factor of approximately 4. As for viscosity changes, the terminal velocity as a function of temperature was calculated to be 43% lower for a representative ilmenite particle at 800°C versus 25°C – see Figure 15. Calculated values of minimum fluidization were determined using Wen and Yu approximation seen in Equation 1 and terminal velocities were calculated using Equation 2. [29]

$$\frac{d_p U_{mf} \rho_g}{\mu} = \left[ 33.7^2 + .0408 * \frac{d_p^3 \rho_g (\rho_s - \rho_g) g}{\mu^2} \right]^{1/2} - 33.7 \dots \dots \dots (1)$$

$$u_t^* = \left[ \frac{18}{(d_p^*)^2} + \frac{2.335 - 1.744 \phi_s}{(d_p^*)^5} \right]^{-1} \dots \dots \dots (2)$$

Table 5. Specifications for the EB at cold flow conditions and calculated hot flow conditions

EB Specifications	
Bed Dimensions	Cylindrical - 8 cm diameter; bed height: 60 cm; Free board: 25 cm
Operating Gas Velocity for coarse OC At 25°C	40 – 60 cm/sec
Calculated Operating Gas Velocity for Coarse OC At 800°C	17 – 26 cm/sec
Fluidization Flow for Coarse OC At 25°C	110 - 165 slpm
Calculated Fluidization Flow for Coarse OC At 800°C (calculated)	47 – 71 slpm

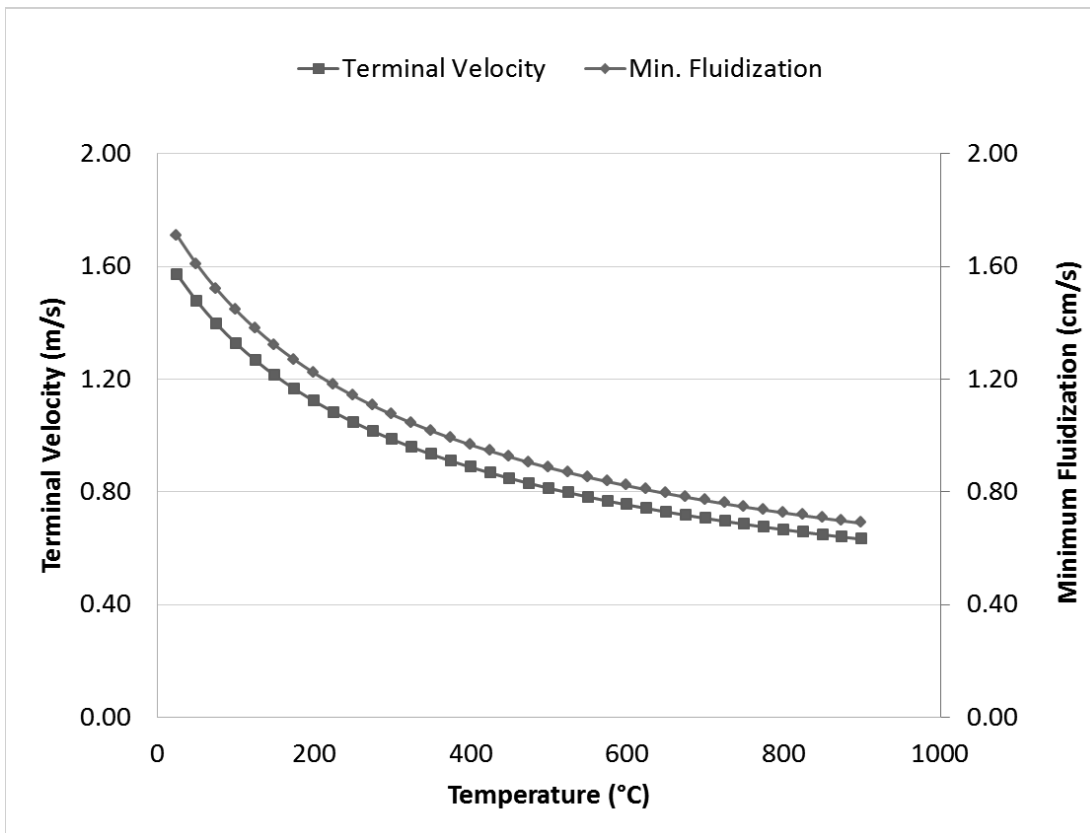


Figure 15. Graph showing calculated changes in terminal velocity and minimum fluidization velocity with temperature for ilmenite particles

With the specifications from the cold flow EB finalized, the hot flow EB was then constructed to the same specifications as the cold flow unit described in Table 5. Minor modifications to the bed length and the freeboard length were made to accommodate the heaters.

Similar to the feed bed, a gas pre-heater was attached to the bottom of the EB unit. The grid plate was made of 325 mesh screen sandwiched between two perforated plates for structural support. External heaters were used to maintain the temperature of the bed at the desired 800°C and carbon dioxide controlled by a mass flow controller was used as the fluidizing gas.

### Design and Construction of the Size Segregation Bed

In the proof-of-concept testing, the size segregation bed (SSB) was able to segregate particles based predominantly on particle density. This characteristic of separation based on particle density should be complementary to the separation in the elutriation bed (EB) which relies on differences in terminal velocities of particles. It's believed that the "Brazil nut effect" [30] potentially plays a role in the movement of the larger char particles to the top of the SSB. From the "Brazil nut effect" study, it was indicated that if the large particles are less dense than their surrounding particles they rise to the top and stay there. This remains true with the SSB unless bed circulation redirects the char particles away from the top.

Testing showed that vertical transportation of char particles was influenced by both the gas velocities and the hydrodynamic fluidization regime being utilized. As discussed previously, segregation is not just due to differences in terminal velocities but more likely due to differences in densities of the materials. Areas identified during initial testing that required design improvements were a) improving the carbon-rich top layer discharge and b) identifying control options for continuous operation. The cold flow system was built to address some of these issues prior to construction of the hot flow system.

The cold flow unit was built using 2.5 cm (1 inch) thick acrylic boards to the internal dimension specifications identified in the proof-of-concept testing as 15 cm wide by 30 cm long with a bed depth of 15 cm. A distributor plate was designed to ensure a pressure drop of at least

7.5 kPa (30 in- $H_2O$ ) so as to ensure a uniform air flow throughout the bed. The distributor plate consisted of holes drilled to a diameter of 0.04 cm (1/64 inches) in a square pattern. Mixed material was fed from one side of the bed while char rich material and cleaned ilmenite exited the top and bottom, respectively, at the other side of the bed. The exit wall of the system consisted of a weir located 6 inches above the distributor plate for the char rich material and a rectangular exit on the bottom for the clean ilmenite. Figure 16 and 17 show pictures of the cold flow system showing inlet, outlet and position of loop seals.

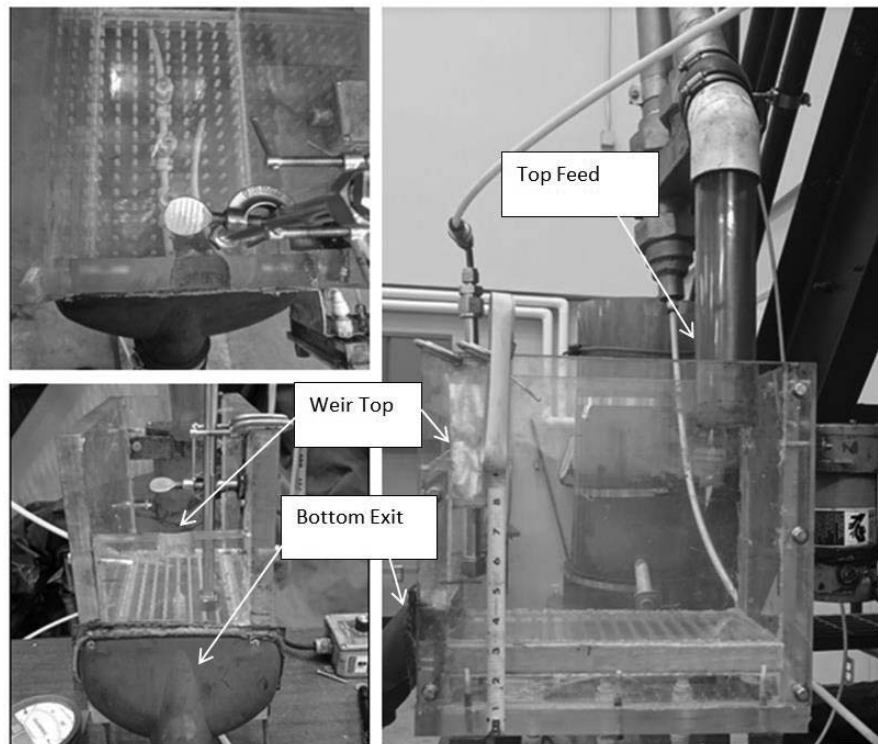


Figure 16. Image showing cold flow SSB system

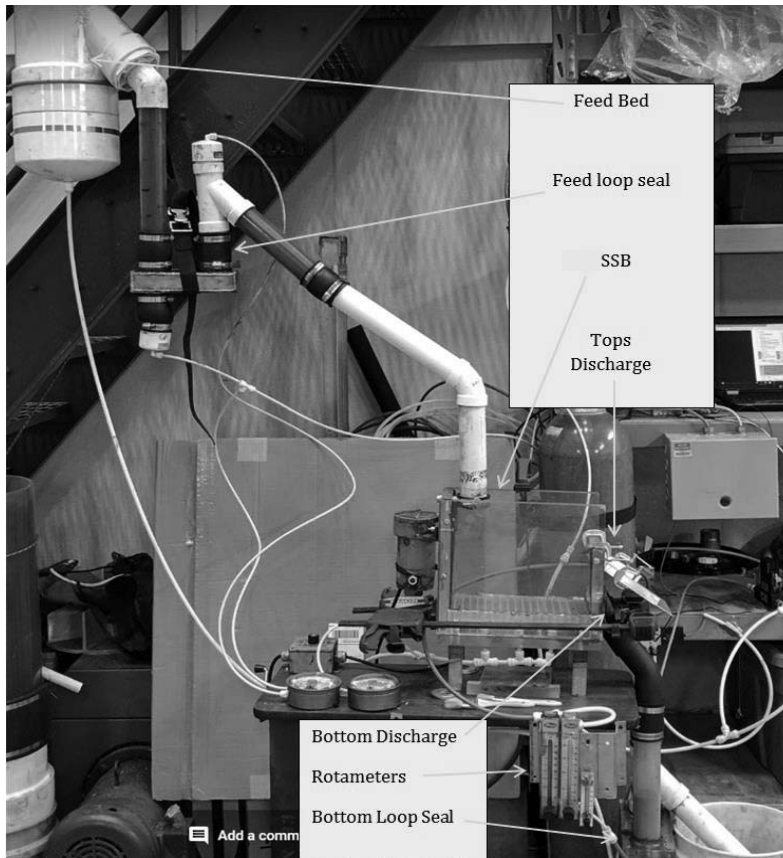


Figure 17. Image showing SSB cold flow set up with rotameters, loop seals, and feed bed

During testing it was observed that separation of materials was possible, however char was dispersed throughout the entire bed and became stuck in certain zones. As a result, the separated char was not exiting the bed in the most efficient manner; overflow of ilmenite was significant. To prevent this, the bed was tilted slightly in the direction of flow to improve directionality of flow and eliminate dead spots that trap char. Tilting had the unexpected advantage of causing the char to “pool” at the bed surface with the lowest elevation (see Figure 18) and creating a char-rich layer that grows as the bed level rises. Also, the char layer location was affected by where bubbles were formed in the OC/char material. For example, by directing more gas flow in the bed towards the walls, the char could be concentrated in the center of the bed making removal much easier. Figure 19 and 20 illustrate the pooling of char as the bed

height increases and the concentration of char to the center of the bed by channeling more air to the walls.

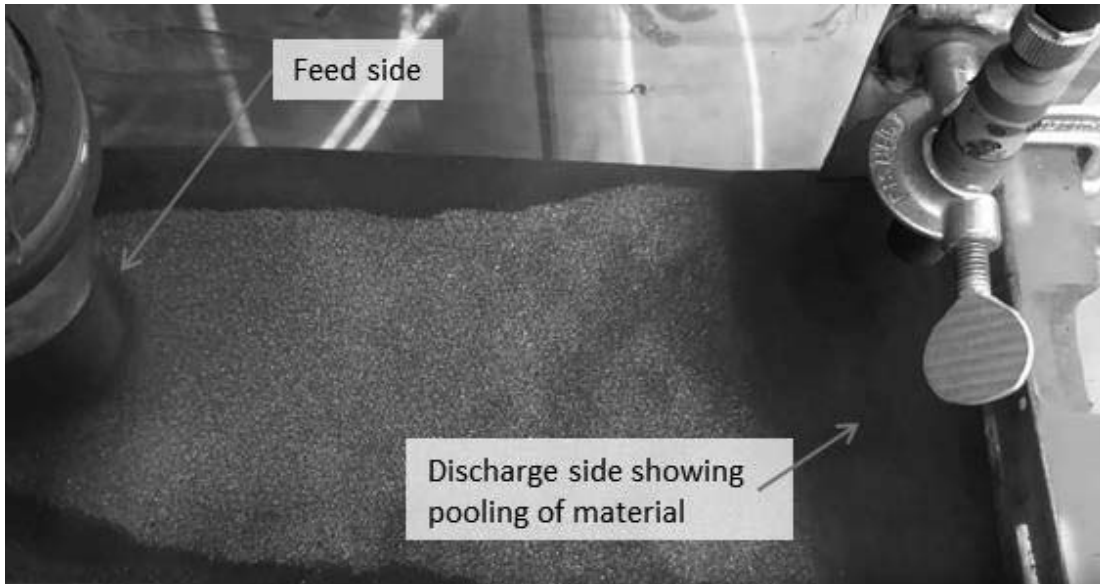


Figure 18. Image showing char segregation

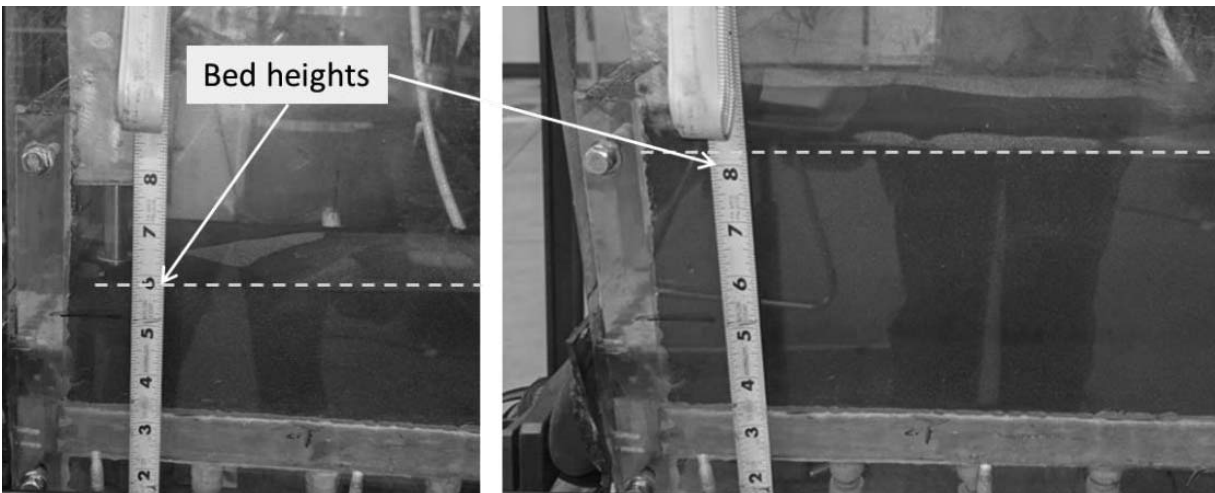


Figure 19. Image showing char building up as bed height rises



Figure 20. Image showing char concentrating in center of bed due to higher air flow at walls

The “pooling” of char ensures a rich char-OC mix can be removed from the system. A control system was designed that consisted of dropping the bed height by 2 to 4 inches in order to allow time for char to concentrate before being discharged at the top. Operating the unit this way allows the SSB to serve as a “polishing surge tank” which prevents fresh feed material from “short-circuiting” the bed. One other advantage of operating the unit this way is that a control scheme can be devised that involves using bed pressure to determine bed inventory. A pressure tap was installed in the bed from the top (see Figure 20) and as the bed level engulfs the inlet of the pressure tap, a small but quantifiable increase in pressure is detected. Placing pressure taps in several locations allows for the bed inventory to be monitored. Also, the material feed rate can be determined through the use of these pressure taps by dividing the weight of material in between them by the time it takes to fill/discharge from one to the other.

Based on the results obtained from the cold flow SSB testing, the final design specifications were acquired and are summarized in Table 6. The results obtained were also corrected for hot operating temperatures of 800°C as with the EB. Viscosity changes are expected to affect the minimum fluidization velocity which is a key factor for the SSB (terminal velocity for the EB). As shown in Figure 15, higher temperatures will also reduce the minimum fluidization by approximately 42%. The corrected gas velocity and fluidization flow are also included in Table 6.

Table 6. Specifications for the SSB cold and hot flow conditions

SSB Specifications	
Bed Dimensions	Rectangular - 15 x 30 cm; Bed depth: 15 cm
Operating Velocity for Coarse OC at 25°C	6 cm/sec
at 800°C (calculated)	2.5 cm/sec
Flow rate at 25°C	160 standard L/min
Flow rate at 800°C (calculated)	~ 20 standard L/min

#### Final Design of PCS System

With the results obtained from cold flow testing, the final design of the PCS system is shown in Figure 21. The schematic shows the feed bed, loop seals, SSB and EB unit. The MFCs are used to control the loop seals and to provide fluidization gas to the beds. Pressure transducers are used as a control strategy to monitor inventory of the respective beds. A cross sectional view of the SSB showing the location of the pressure taps, char exit, and ilmenite exit can be seen in Figure 22.



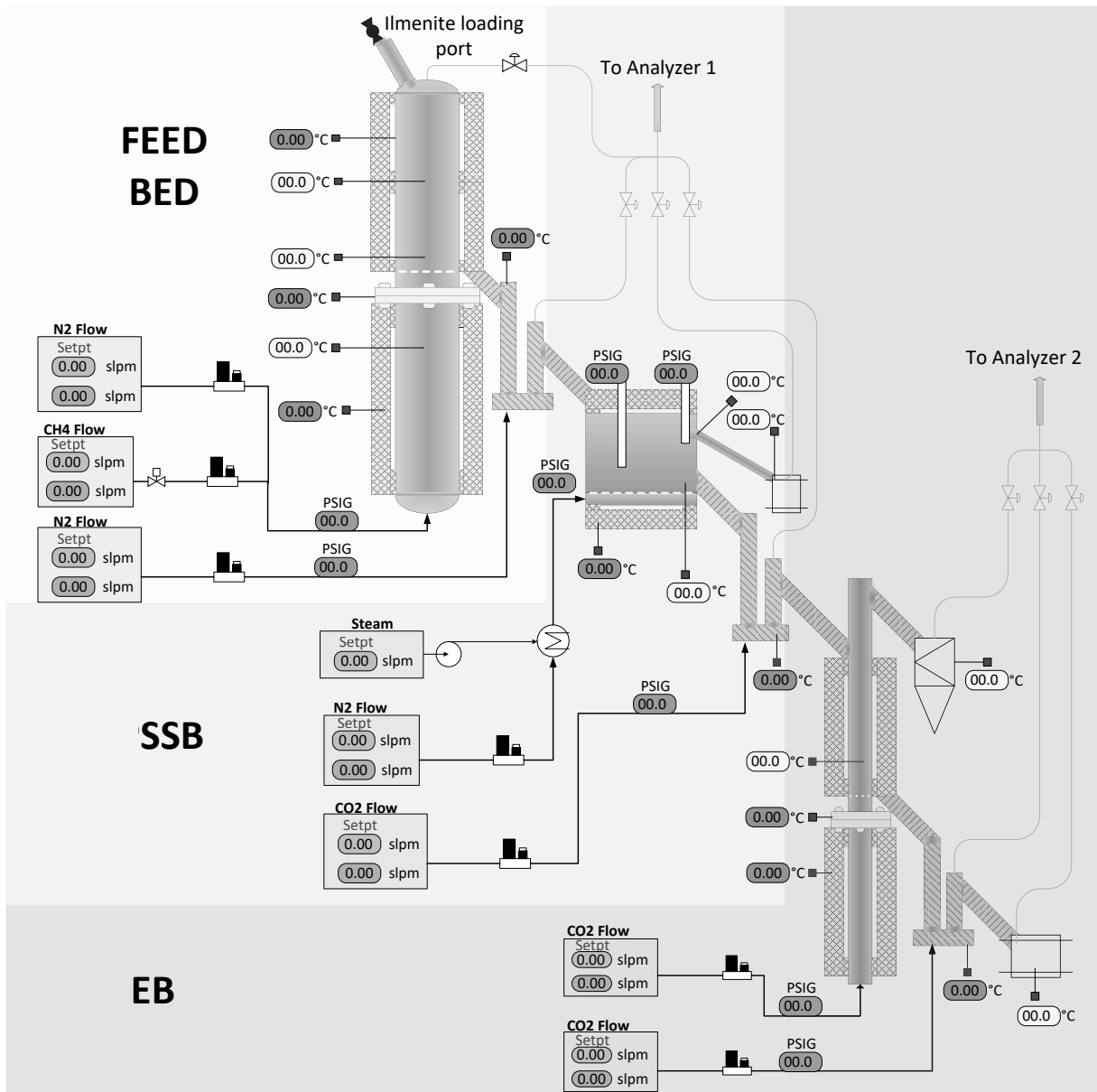


Figure 21. Final control schematic and configuration of PCS system

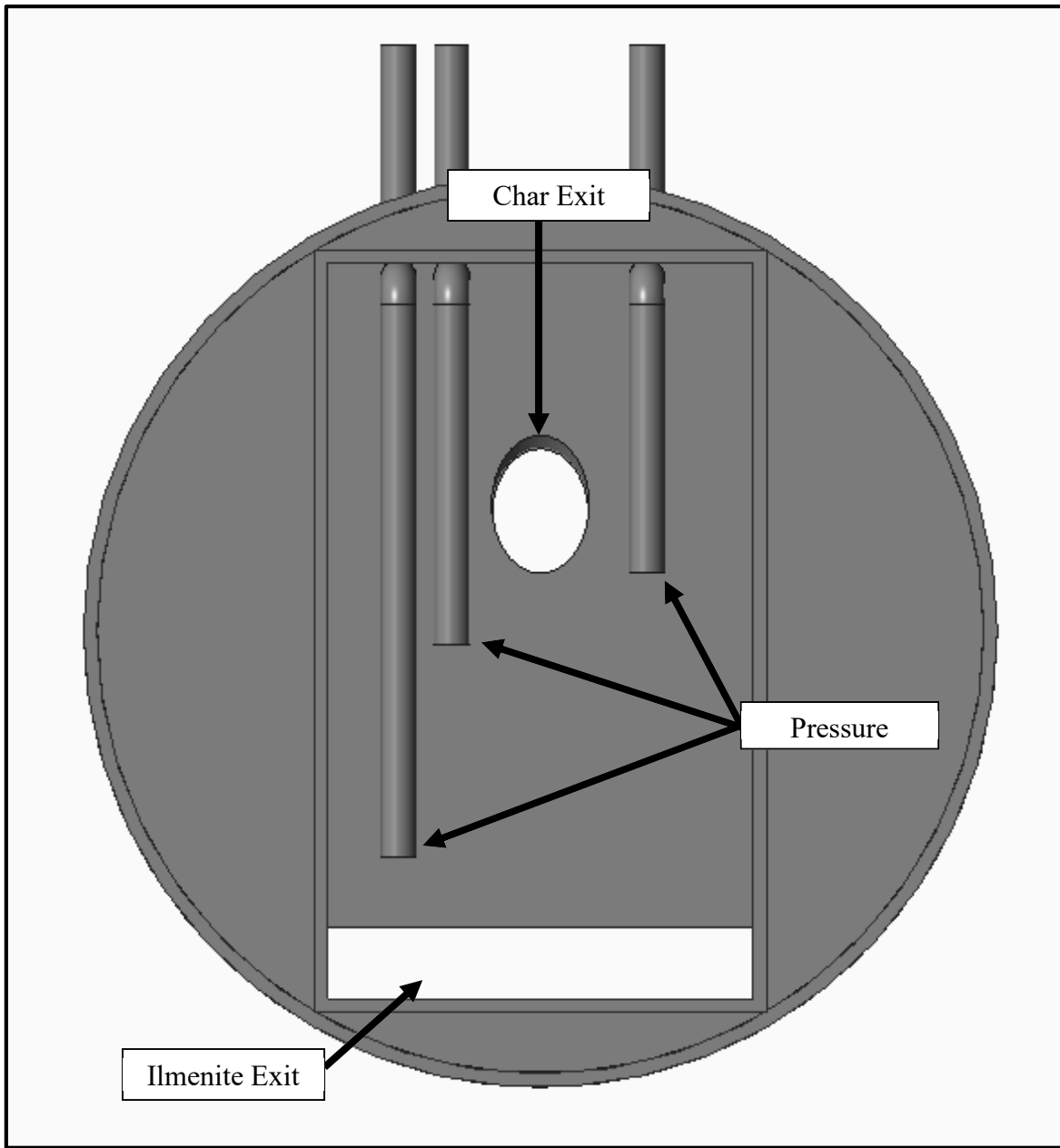


Figure 22. Cross sectional view of SSB

A picture of the completed fabrication of the hot flow unit can be seen in Figure 23. All beds and loop seals are heated using ceramic heaters or high temperature heat tape. Cyclones and fabric filters are used to capture char-rich material removed from the respective beds.

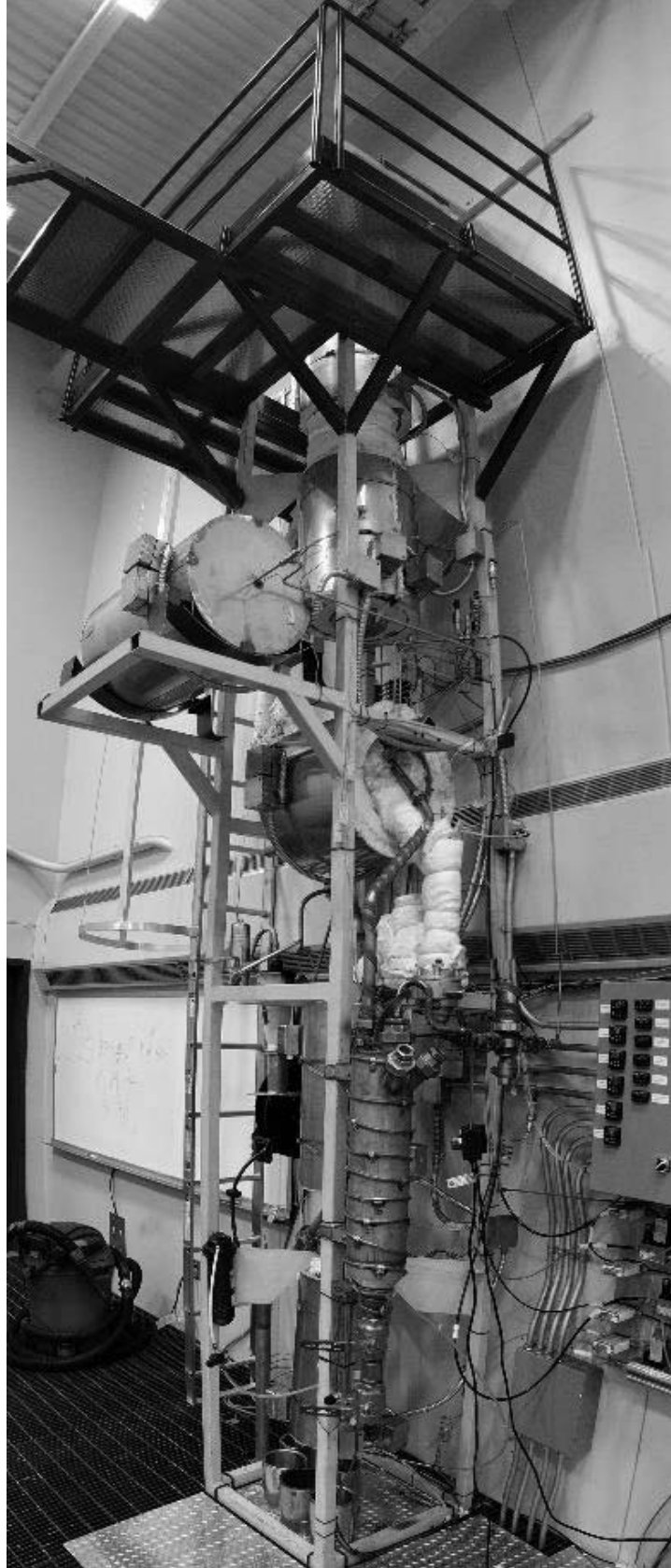


Figure 23. Completed hot flow unit

## Process Control

In order to partially automate operation, a control system was created using LabVIEW software. Images of the system control and heater control panel can be seen in Figures 24 and 25, respectively. The control panel allows for operators to easily view pressures, temperatures, material feed rates, and bed inventory. Additionally, valves can be opened or closed to allow for gases to flow to a laser gas analyzer (LGA) to determine gas composition in various locations. Alarms were also created to alert operators of unwanted pressure or temperatures in several locations. A data logging system was also implemented in order to gather details about various parameters for post run analysis.

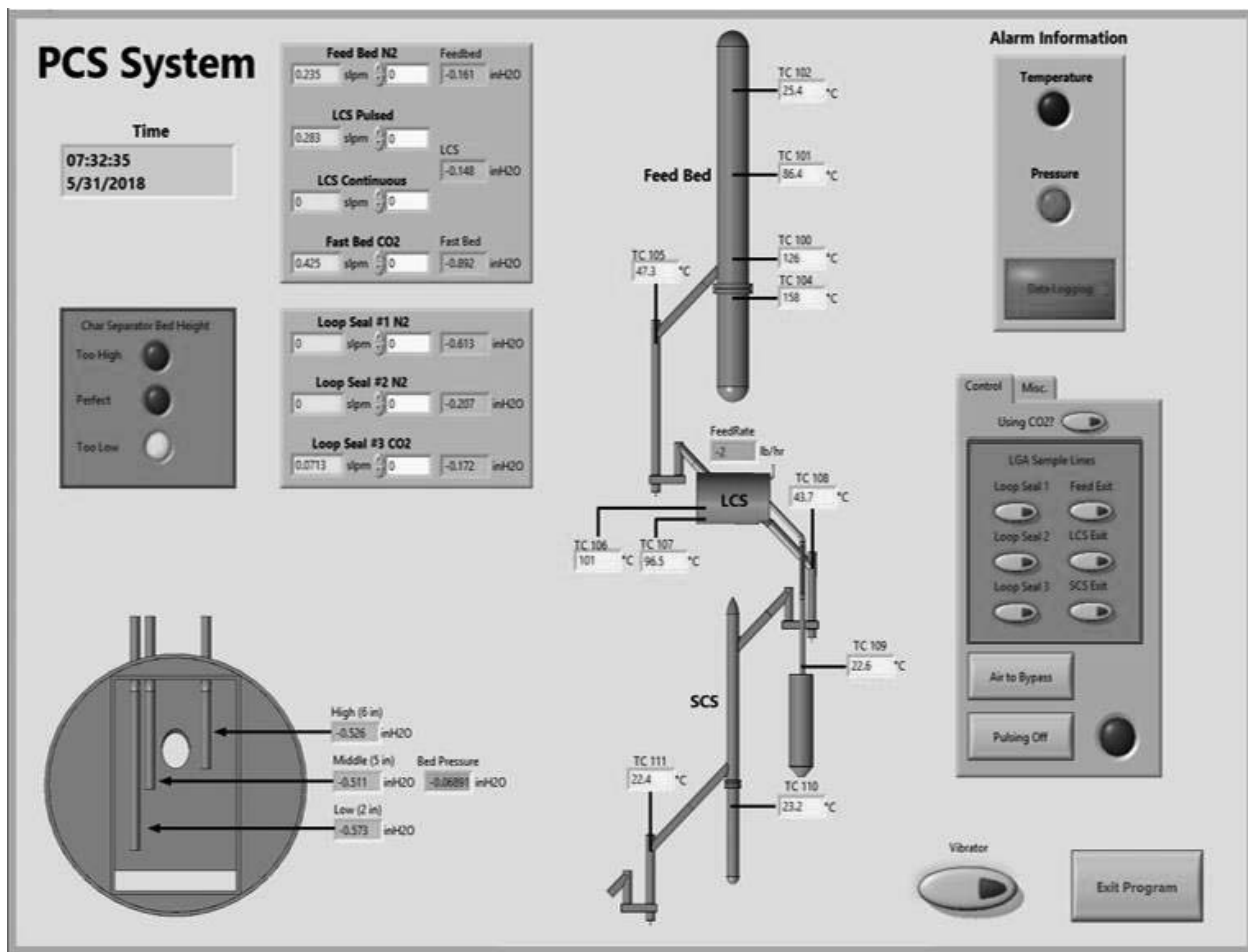


Figure 24. System Control

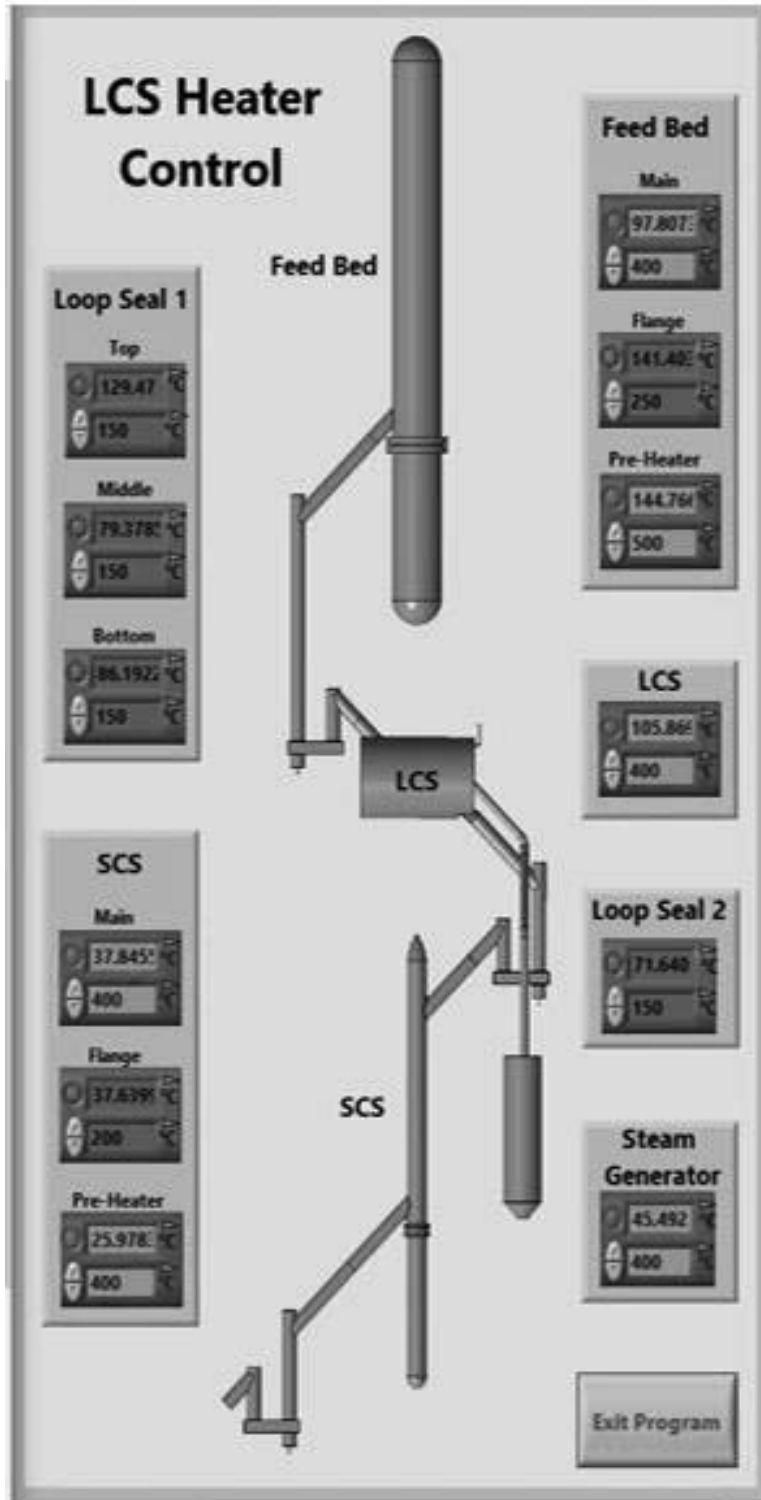


Figure 25. Heater control

## CHAPTER IV

### COMPONENT TESTING OF THE HOT FLOW SYSTEM

This section will look at the char segregation results obtained during operation of the EB and SSB in the hot flow unit at ambient temperature. Four tests were performed (two EB and two SSB). Tests 3 and 4 were done on the SSB and EB respectively using best practices and control methods developed during previous testing and shakedown (Test 1 and 2). First, we will discuss results obtained from Test 3 and 4 before discussing Test 1 and 2.

#### Test 3 – SSB testing with 0.5% char/OC mix

A 91 kg (200 lb.) ilmenite sample was mixed with 454 g (1 lb.) of prepared char (Tables 2 and 3). The batch was prepared by mixing smaller batches of 9 kg ilmenite with 45 g of char. Figure 26 shows initial char vs OC size distribution with approximately 34% of the char particle size distribution (PSD) overlapping with the ilmenite PSD. The operating conditions during testing of the SSB are summarized in Table 7. During operation, the feed rate to the bed was kept constant at approximately 41 kg/h (92 lb./hr), and the cleaned ilmenite was withdrawn from the unit by turning the bottom loop seal on and off at feed rates of approximately 93 kg/h (205 lb./hr). The on/off trigger for the bottom loop seal was based on how long – approximately 3 minutes – char-rich OC had exited from the top discharge of the SSB. Figure 27 shows step wise operation of the bottom loop seal and top discharge.

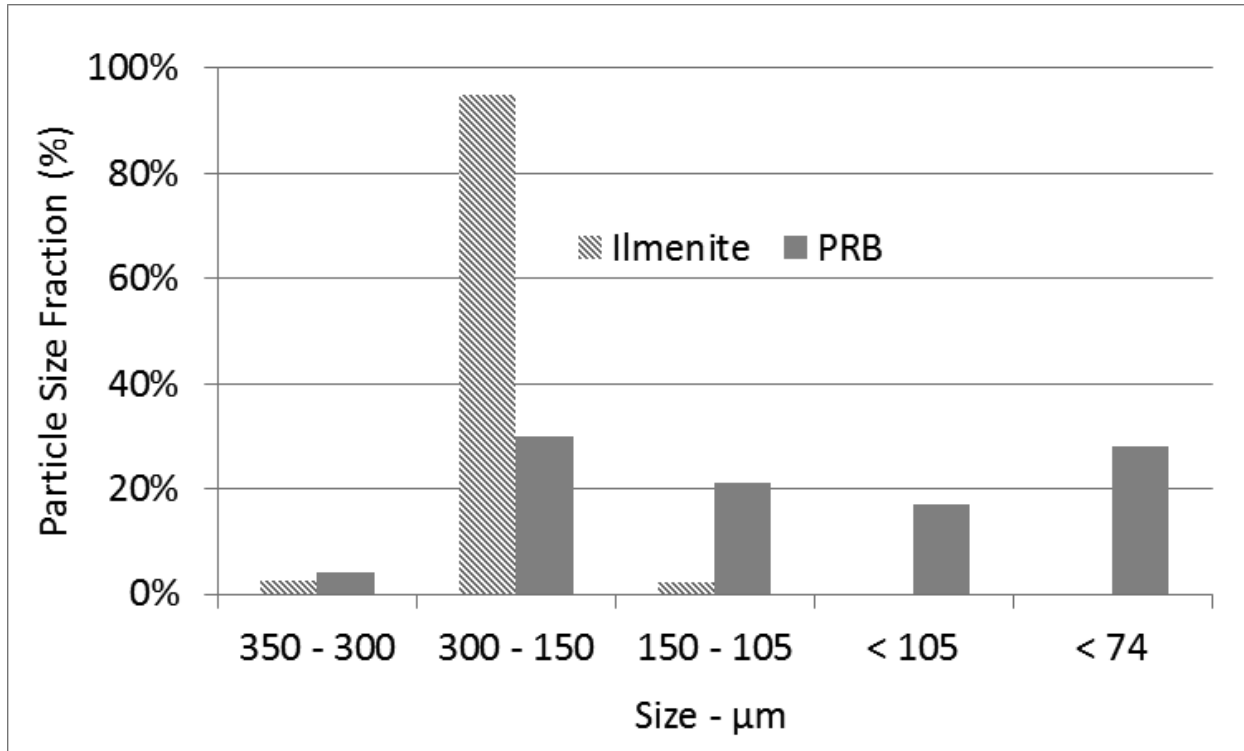


Figure 26. PSD of char and ilmenite used during test 3

Table 7. SSB operating conditions during test 3 of cold flow work.

Test Conditions	
Total average Flow	84 slpm
Ilmenite	90 kg
Char	0.45 kg

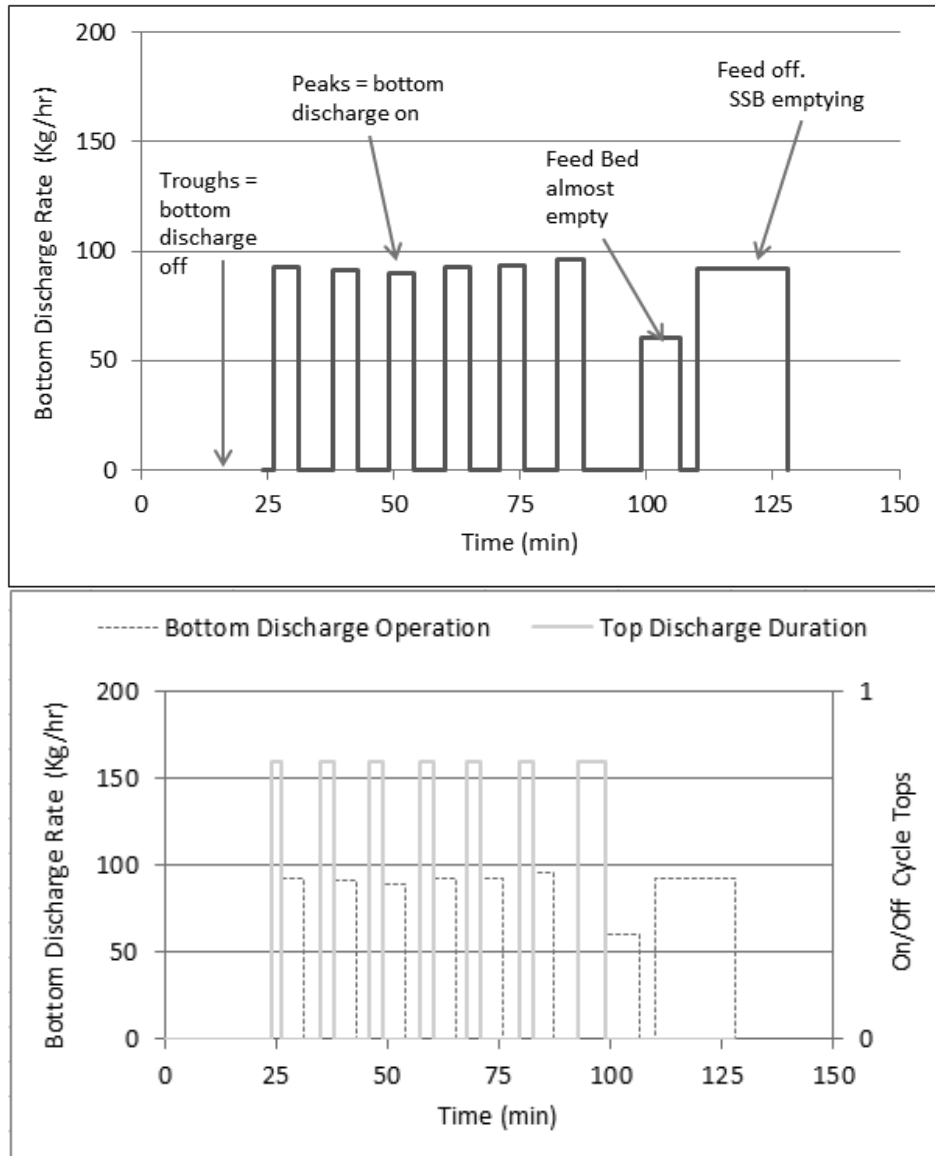


Figure 27. Graph showing test 3 operation of the SSB bottom loop seal (top) and top discharge (bottom)

From 0 to 25 min, the bottom loop seal and bed are filling. It takes approximately 20 kg of ilmenite to fill the system. During fill up, fluidization and vibration are turned on to reduce the amount of char that is “lost” to the bottom loop seal. Once the bed is full (a bed height of 15 cm) material starts exiting through the top discharge, and a 3-minute timer is started. Timer duration is based on previous testing. At the 3-minute mark, the bottom loop seal is turned on at double the feed rate to drop the bed height to approximately 10 cm. The cycle is then repeated. Close to



the 100-minute mark, the feed bed is almost empty, so the top discharge duration is extended to ensure all the segregated char is discharged. The bed is then emptied and the bottom ilmenite saved for Test 4.

Final tops-bottom split is shown in Figure 28 along with the char fractional removal efficiency for each size fraction and a total removal efficiency of 77%, with a 2%/98% split for the tops/bottom discharge. The top was sieved into four size bins and analyzed using a total carbon analyzer. The results obtained were corrected for the carbon content of the char – see Table 3; to determine the percent by weight char in the ilmenite.

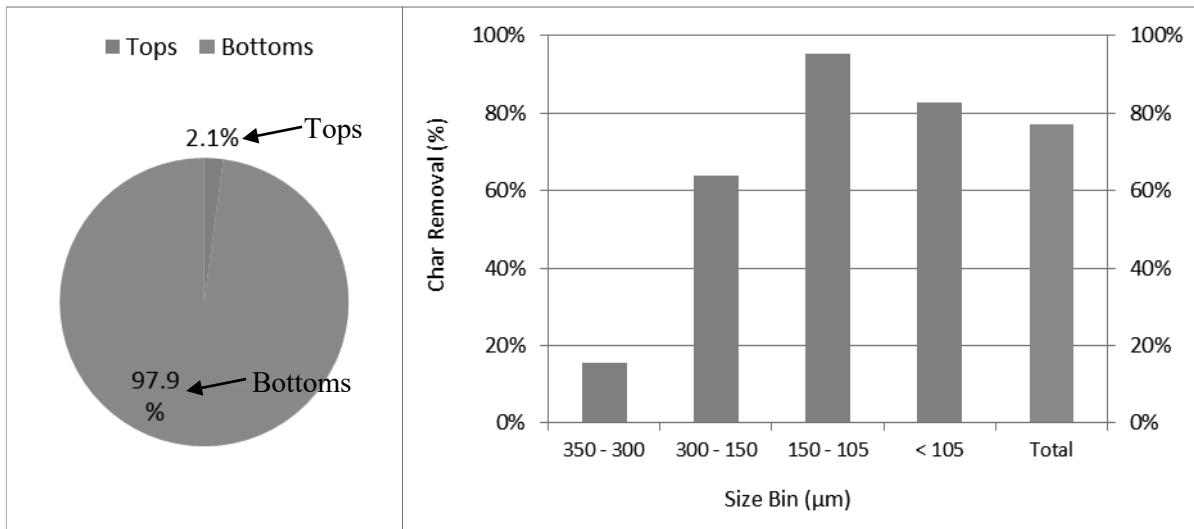


Figure 28. Chart showing tops/bottom split (left) and char removal efficiency (right) for Test 3

Char removal efficiencies were calculated based on amount of char in feed. While the results suggest the SSB is less efficient for coarser particles ( $> 300 \mu\text{m}$ ), this result may be due to the large amount of ilmenite in this size fraction. Recall from Figure 26 that the coarse loading of the char was low and overlapped significantly with the ilmenite. Consequently, the total amount of char in this size range is very small to begin with. Moreover, based on discussions with GE Power, the use of finer coal for CLC to improve conversion rates will reduce the occurrence of unburnt char in large size fractions.

The char concentration in the tops discharge was 13 percent, up from 0.5 percent in the feed, an increase by a factor of 26. Such a high increase is due to the density difference between the char and OC and also from the initial PSD of the ilmenite/char used. The SSB is good for separating large particles with lower densities from high density and large particles. However, very fine particles are also separated due to their lower terminal velocities. It's expected that conditioned/cycled OC will have a finer OC distribution which will result in the tops discharge having a higher OC content than above. Another factor that would directly impact the tops discharge is the operation mode. A longer duration for the tops discharge will also result in more OC being removed from the tops discharge and affecting the overall tops/bottom split.

#### Test 4 – EB Testing of Test 3 Bottoms

The bottoms from the SSB were cycled through the EB unit as a “polishing” step to improve overall separation. The EB unit was operated at a bed velocity of 60 cm/s for an operating flow of 160 standard liters per minute. This velocity was chosen following results obtained from Test 1. During operation the feed and discharge loop seal were operated to maintain an EB pressure drop of approximately 15 kPa (60 in. water) which corresponds to a bed inventory of approximately 3 kg and bed height of 28 cm. The bed pressure drop was used to maintain inventory in the bed. Figure 29 summarizes the results obtained. During operation, the feed rate through the system was approximately 31 kg/h – slightly lower than for the SSB, even though the same loop seals and operating conditions were used. This is attributed to the lower concentration of fines in the OC/Char mix used from Test 3. During hot flow operation, focus will be on bed inventories to minimize the effect of changing feed rates.

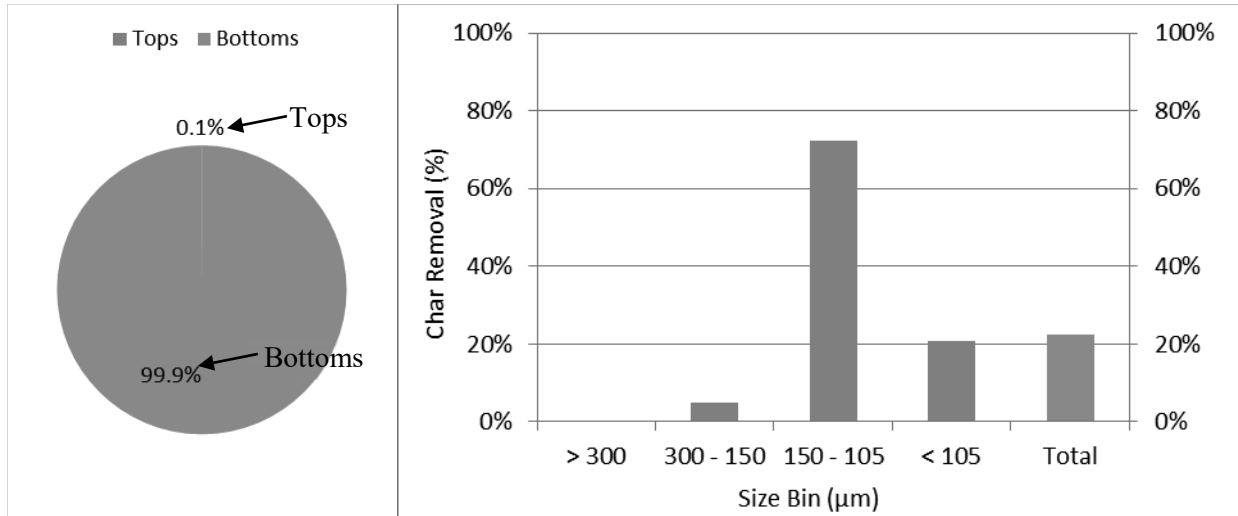


Figure 29. Chart showing tops/bottom split (left) and char removal efficiency (right) for Test 4

The tops loading of the EB was very small – 0.1% due to the absence of fines in the ilmenite used. The total char removal is 22 percent with most of the separation occurring in the 150 to 105  $\mu\text{m}$  range. The EB separates particles as a function of their terminal velocity differences and so the absence of fine OC with terminal velocities that overlap with the char results in a low amount of elutriate. The combined removal efficiency of running the PSSB and EB in series was 82 percent.

### Test 1 – Optimizing EB Performance

Test 1 focused on optimizing the EB to determine optimum cold flow operating conditions which will then be corrected to account for temperature. For these tests, 8 test samples comprising 7 kg of ilmenite and 70 g (1 percent) of activated carbon (Table 2 and 3) were prepared and ran through the EB at different bed velocities. The elutriate collected was then analyzed using a carbon analyzer. The results were used to determine optimal bed velocities and separation efficiencies for the EB during cold flow operation. The data will then be corrected to develop the test conditions for the hot flow unit. Figure 30 shows the total material elutriated and percent char removed as a function of bed elutriation velocity.

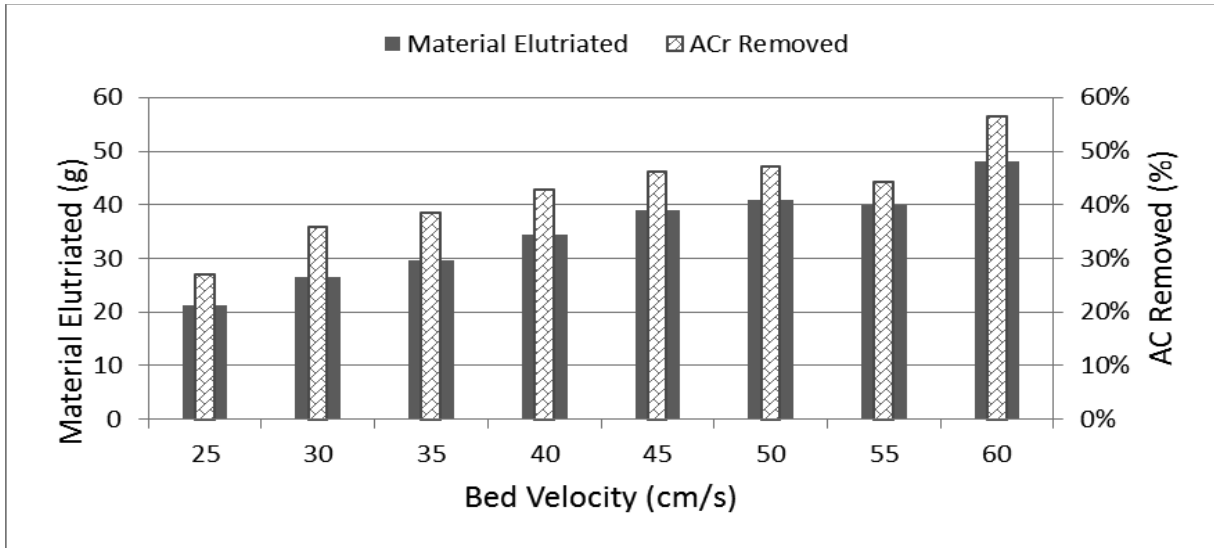


Figure 30. Total material elutriated and corresponding char removal for Test 1

The data in Figure 30 show that as the velocity increases the amount of material elutriated increases up to approximately 45 cm/s at which point the elutriate and char removal level off. A further increase is observed for the 60 cm/s test condition. The bump at the 60 cm/s is due to the char reaching terminal velocity for the smaller particles as noted by the size distribution of the char being elutriated. This is better illustrated in Figure 31 which shows carbon removal as a function of size fraction loaded. As the velocity increases, finer carbon (less than 150  $\mu\text{m}$ ) is removed significantly with removal rates of over 80% observed at 60 cm/s. The larger char size fraction (300 – 150  $\mu\text{m}$ ) stays the same at 40 cm/s to 60 cm/s. Based on these results, optimum cold flow operating conditions are bed velocities from 40 cm/s to 60 cm/s for an OC/char mix with similar densities.

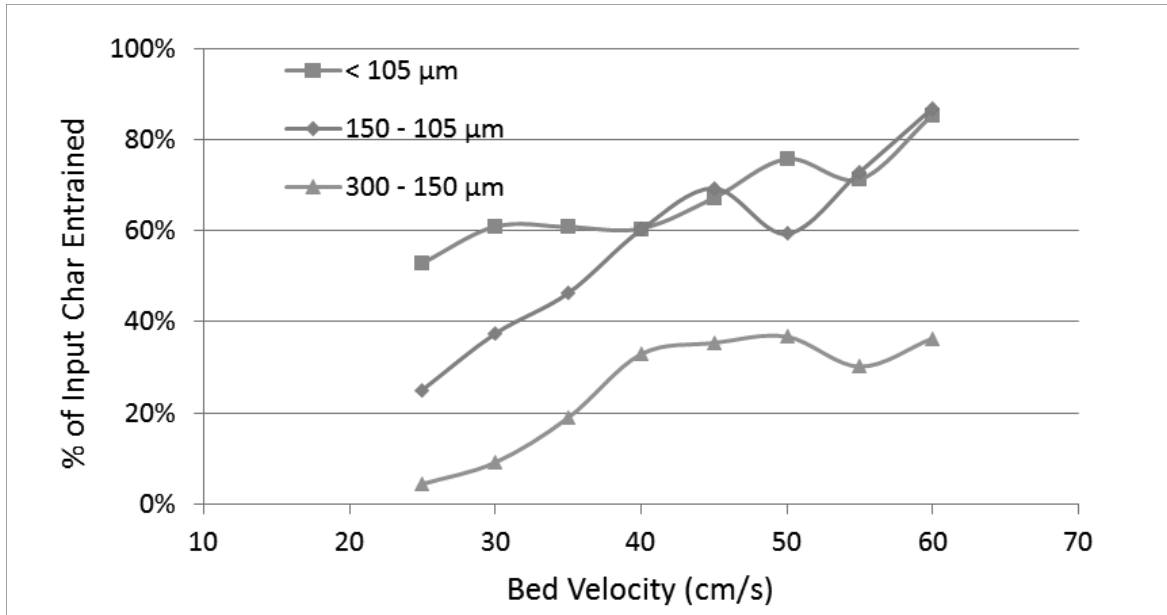


Figure 31. Char removal efficiency as a function of particle size and bed velocity

#### Test 2 – Optimizing SSB Performance

For test 2, three 23 kg ilmenite samples were prepared at AC concentrations of 1, 2 and 0.5 percent; and fed in that order through the SSB system consecutively. Due to memory effects from the loop seals and bed (carbon material retained in the different units), the results were combined and the feed composition treated as a composite of 1.2 percent AC. On average, 68 kg of ilmenite containing 820 g of activated carbon (AC) was fed through the SSB unit. To reduce the memory effects, fresh ilmenite was fed through the system at different intervals to “flush” out char. The operating conditions were similar to Test 4, and visual observation of the char layer was used as the control method for the test. Optimized operating practices such as dropping the bed height to increase char concentration, timing the duration of the tops discharge, and monitoring bed inventory to account for changes in feed rate were established during this test.

The tops discharge collected from this test was analyzed to determine the carbon content of the tops discharge. The results obtained are summarized in Figure 32 showing a tops/bottom split of 2.2%/97.8% respectively and a total char separation of 45 percent. The tops/bottoms

splits include the fresh ilmenite added at separate intervals to flush out char. Consequently, the results presented are for an average separation performance calculated from the amount of activated carbon fed and removed from the tops discharge.

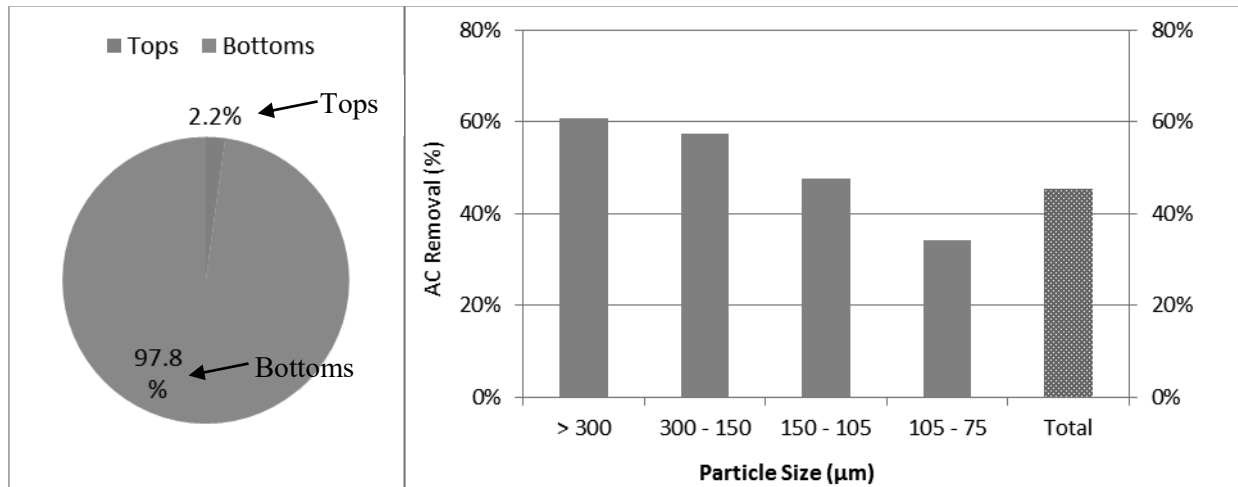


Figure 32. Chart showing tops/bottoms split (left) and char removal efficiency (right) for Test 2

34 percent of the AC material used was in the “> 150  $\mu\text{m}$ ” range (Table 7). AC’s “> 150  $\mu\text{m}$ ” size bin was coarser than the char used in Test 3. This explains the better separation observed for the larger size fraction than with the char material in Test 3. Separation observed in the finer fractions was also significant with over 30% observed for the “< 150  $\mu\text{m}$ ” size bins.

This test showed the potential of the SSB to achieve the bulk of the char segregation but also served to provide insight on possible control options for the hot flow case. Operating practices such as dropping the bed height to increase char concentration, timing the duration of the tops discharge, monitoring bed inventory to account for changes in feed rate, and using pressure to determine bed inventory were all developed as part of this test campaign.

## Summary of Test Results and Implications for the Hot Flow Design

The results obtained during component testing of the cold flow PCS system were used to finalize the design of the hot flow PCS System. The impact can be sub-divided into two main areas: operating conditions for hot flow testing and control of hot flow unit.

### *Operating Conditions*

Cold flow testing identified operating conditions – flow rates and velocity – for the SSB and EB units. These were then corrected for temperature to obtain starting operating conditions for hot flow testing. Table 8 summarizes operating conditions identified.

Table 8. Operating conditions for SSB and EB units

	<b>EB</b>	<b>SSB</b>
<b>Solids Residence Time</b>	1 minute	6 minutes
Superficial Gas Velocity		
At 25°C	40 – 60 cm/sec	6 cm/sec
<b>At 800°C (calculated)</b>	<b>17 – 26 cm/sec</b>	<b>2.5 cm/sec</b>
Fluidization Flow Rate (std. L/min)		
At 25°C	110 - 165	80
<b>At 800°C (calculated)</b>	<b>13 – 19</b>	<b>10.5</b>

### *Control of Hot Flow Unit*

The biggest challenge with hot flow testing is the absence of visual feedback on how effective the units are at segregating char from the OC. During cold flow testing, a key objective was to determine methods to control unit operations without compromising effectiveness of segregation. For the EB, the separation principle is terminal velocity – a fast separation method that depends on bed velocities; and disengagement height. Bed velocities were determined during cold flow testing and adjusted for temperature (see Table 8). Disengagement height is a

function of bed inventory. During EB cold flow testing, bed inventory was successfully monitored using bed pressure drop.

For the SSB, the separation principle is such that particles of lower density get segregated to the top of the bed due to differences in size and density. Cold flow testing established that by cycling the bed height through a high (discharge) and low level, we can minimize the amount of ilmenite that is discharge/entrained with the segregated char. The challenge lies in monitoring the bed height at temperatures of 800°C. This will be achieved by installing a thermocouple at the bed discharge and using pressure taps at desired bed heights to control the bed inventory. The thermocouple will detect when material is flowing from the bed; the pressure taps will be used to identify the bed inventory/height.



## CHAPTER V

### HOT FLOW RESULTS AND DISCUSSION

Upon completion of component testing, the next step was to begin testing of the integrated system. Before ramping the system to 800°C, it was important to first discover any possible challenges associated with elevating temperatures from 25°C. In order to determine how the system would react to increasing temperature, tests were first conducted at temperatures of 300°C - 400°C. After various tests, several challenges were identified and mitigations strategies were implemented which are listed below.

#### Challenges and Mitigation Strategies

**Challenge: Inconsistent loop seal feeding** – During the operation of the loop seals it was observed that desired feed rates would change unexpectedly, making operation difficult.

Causes:

- Cold flow testing showed that the original loop seal design fed better at flow rates greater than the desired operating window
- It was found that uneven heat distribution within the feed leg would cause the loop seals to change feed rates due to changes in gas viscosity
- Unknown instantaneous feed rates during runs made operation of the loop seals difficult and calibration before each run utilized too much material

Mitigation strategies:

- A re-design of the loop seal made it less sensitive to changes in gas flow during runs
  - The new design consisted of a plenum that stretched across the entire length of the loop seal body
  - A change in the distributor plate design from a mesh screen to a perforated plate created a larger pressure drop across the distributor plate
- In order to maintain an even heat distribution, the loop seals were wrapped with thicker insulation to prevent heat loss during transportation of the solids
- Heat tapes that were found to be loosely wrapped were re-adjusted in order to allow for better heat transfer to the loop seals
- The LabVIEW programming was optimized to allow for better operation of the loop seals
  - A program was created that could be used to determine the approximate feed rate of the loop seals in real time
  - A graph buffer program was created to take the moving average of the pressure to make graph lines smooth
  - Differential pressure calculations were integrated into LabVIEW in order to better determine the bed height of the material in the SSB

**Challenge: High/inconsistent pressures and talk between units** – During operation it was observed that pressure transducers were maxing out when the SSB was full. The high pressure made it so that when gas flows were changed in one unit, pressures would change proportionally in other units.

Causes:

- Higher gas flows that were used with the coarse oxygen carrier resulted in a larger pressure build up within beds
- Exhaust lines from each unit were originally designed to be tied together in order to simplify the exhaust exit
- It was found that water build up within the filter on the feed bed exhaust would fill up with evaporated water, restricting gas flow and resulting in a higher pressure drop across the filter
- The original filters had a relatively small cross sectional area, resulting in a fast accumulation of fine particles, resulting in a greater pressure drop

Mitigation strategies:

- A water bubbler was added to the exhaust of the last loop seal in order to relieve any pressure build up in the system
- The diameter of the exhaust lines was increased in order to create less of a pressure drop through the exhaust
- The new exhaust lines for each unit were ran individually to the exhaust system of the building in order to isolate the pressures from each other
- Due to the low gas flow rates in the feed bed, the filter was able to be removed and a condenser was added to capture moisture
- The old cyclone on the EB was removed and replaced with a lower efficiency cyclone in order to reduce pressure drop
- The filter located after the cyclone on the EB was replaced with a Donaldson filter that consisted of a larger surface area, allowing for a greater amount of particle build up without a significant increase in pressure

- The filter on the exhaust of the SSB was replaced with a bag filter with a larger surface area

**Challenge: Long heat up time** – When attempting to heat up to desired temperatures it was found that a significant amount of time was needed (over 10 hours). This heat up time wouldn't be of concern in a continuous system, however, with a batch system its necessary to heat up and cool down for each run in order to load material.

Causes:

- The large amount of material located within the feed bed made heat transfer to the center of the bed slow
- It was found that some heat loss was occurring at the top of the feed bed due to an insufficient amount of insulation

Mitigation strategies:

- A thicker layer of insulation was added to the top of the feed bed to reduce heat loss during heat up
- In order to allow for a longer heat up time, a decision was made to begin heating up the material overnight rather than during working hours
  - This longer heat up time allowed for an even heat distribution of the material
  - Heating up overnight also allowed for more time during the day to run and do post analysis which increased the total amount of runs that could be conducted each week

Results for Coarse (230  $\mu\text{m}$ ) Ilmenite at  $\sim 300^\circ\text{C}$

Once the challenges associated with operator elevated temperatures were addressed, tests were conducted to validate that the separation of char is possible at approximately  $300^\circ\text{C}$ . Table 9 shows the operating conditions for each test as well as the split (percent OC recycled) and total char removal percentage. Due to protection of intellectual property, details regarding the fluidization regimes are not able to be discussed and will therefore be referred to as fluidization regimes “A”, “B”, and “C”.

Table 9. Test Conditions for 230  $\mu\text{m}$   $300^\circ\text{C}$  tests

Run	1	2	3	4	5
Char-to-OC, %	0.54	0.78	0.48	0.87	0.55
Feed Average, lb/hr	92	68	89	NA*	189
Fluidization Regime	C	C	A	B	B
LCS Temperature, $^\circ\text{C}$	320	304	302	NA*	349
Tops-Bottom Split, %	32%	10%	19%	10%	19%
Total Removal, %	83%	61%	65%	59%	54%
Char pot loading	1.4%	4.5%	1.6%	4.9%	1.4%
Clean OC loading	0.14%	0.35%	0.23%	0.41%	0.35%

NA\* - Data not available due to temporary issues with data acquisition software

The effects that the flow regime and split have on the overall char removal can be seen in Figure 33. Results show that fluidization regime “C” allowed for the highest separation of 83% char removal with a 32% split. This split was slightly higher than the target of 20% so a test of the same conditions was repeated and results show a 60% removal with a 10%. It can then be said that with a 20% split the char removal would most likely be between 60-83% for fluidization regime C. All tests were performed at an average bed velocity of approximately 2.5 cm/s which was found to be the minimum fluidization for the coarse ilmenite.

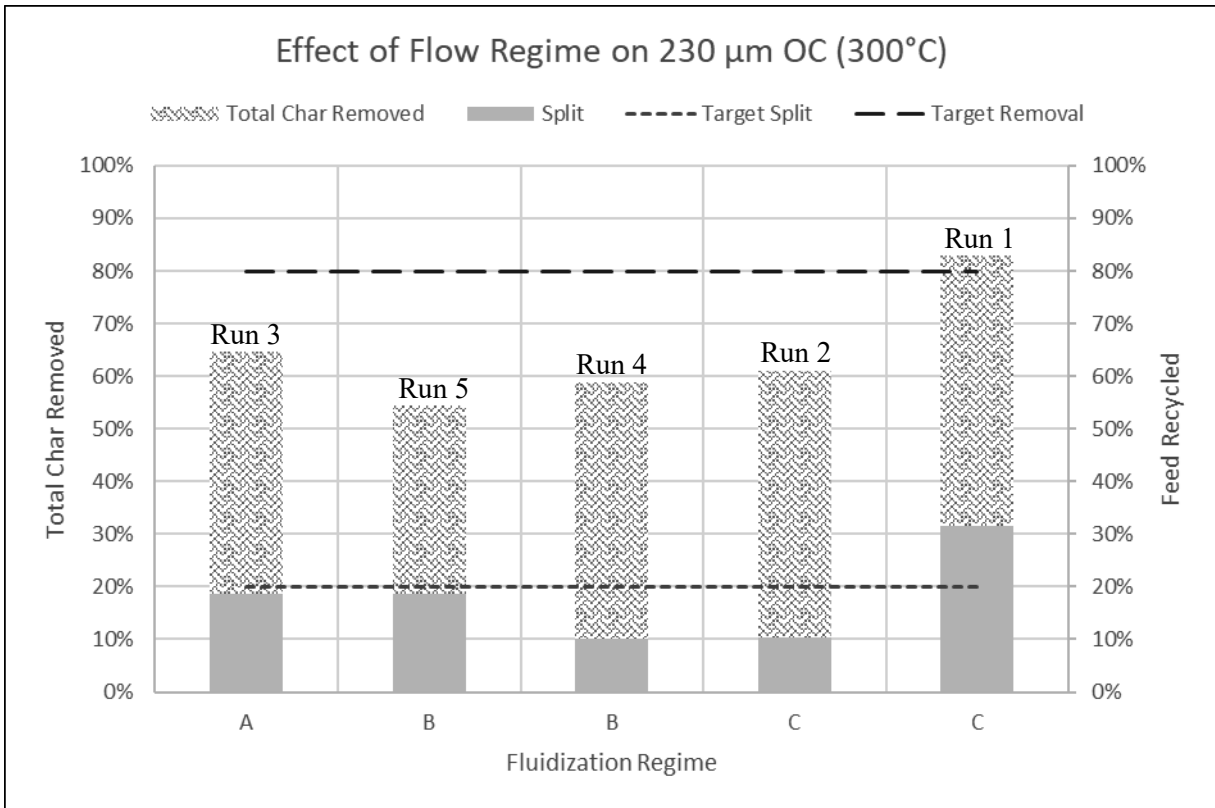


Figure 33. Char removal for 230 μm OC

In order to see if the SSB is effective at removing char of all size ranges, an analysis of the carbon percentage for each size range was conducted and results are shown in Figure 34. Results show that the SSB is capable of separating all size fractions of carbon rather than just coarse size fractions. It can be seen that for all but one condition, more than 50% of the carbon in each size bin is concentrated in the tops. This implies that removal of the EB from the PCS in future work is possible and by doing so would reduce the total amount of gas required for effective separation.

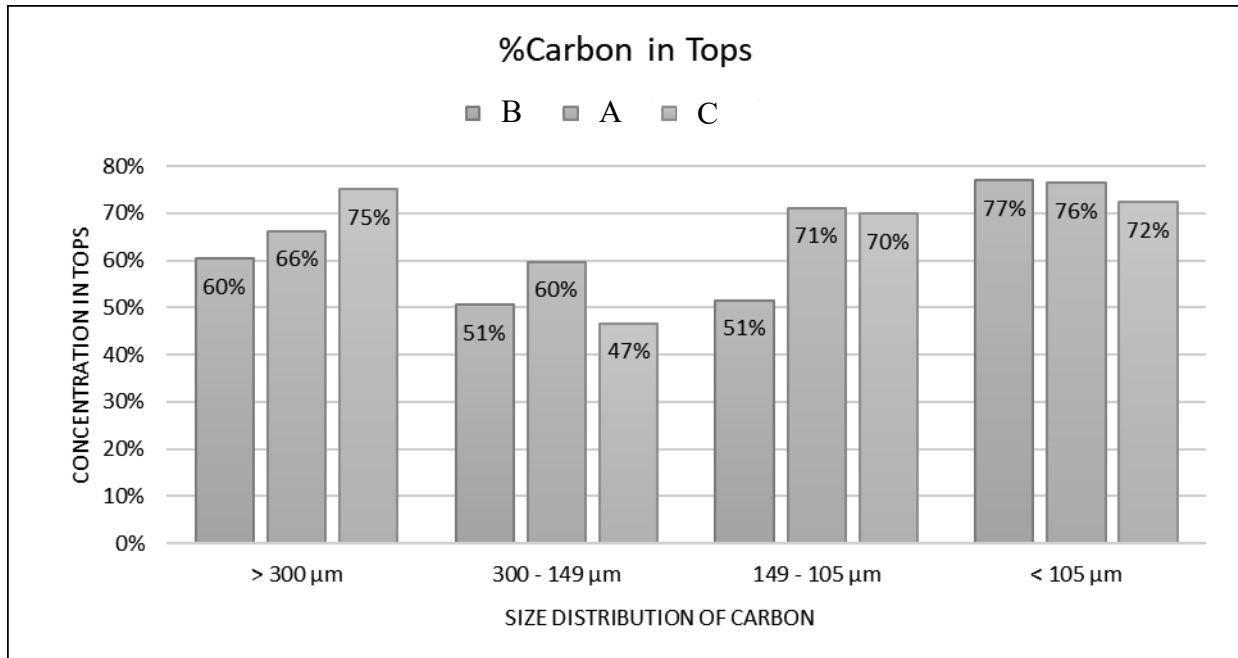


Figure 34. Percent Carbon in each size range

Results for Fine (94 μm) Ilmenite at ~ 300°C

For the fine ilmenite testing, run conditions can be seen in Table 10 and the overall char removal for each fluidization regime can be seen in Figure 35. Results show that good separation only occurs when a high split is achieved, regardless of the fluidization regime. A larger number of runs were performed using fluidization regime “C” since it proved to have highest separation using the coarse ilmenite. Lower separation occurred due to the fact that the minimum fluidization velocity needed for the fine ilmenite was not high enough to bring the majority of the char to the top of the bed. It was observed on a separate cold flow unit that when higher gas velocities were used in attempt to migrate the char to the top of the bed, back mixing would occur, preventing any separation.

Separation for each fluidization regime on the fine ilmenite proved to be poor, however, the size distribution of the fine ilmenite is not representative of what would be seen in an actual CLC system. Rather, the size distribution used represents an exaggerated level of attrition

(discussed previously). These tests were necessary to demonstrate that char removal is possible (with high splits) even under high levels of attrition.

Table 10. Test Conditions for 94  $\mu\text{m}$  300°C tests

Test	1	2	3	4	5	6	7	8	9	10	11
Char-to-OC, %	0.8	0.7	0.7	0.9	0.6	0.7	0.7	0.6	0.7	1.03	1.55
Feed Average, lb/hr	90	67	36	27	100	124	150	126	139	34.2	70
Avg Bed Flow, Umf	2.2	2.6	2.6	1.8	2.8	2.7	2.7	2	2	2.5	2.5
Fluidization Regime	A	B	B	C	B	C	C	C	C	C	C
LCS Temperature, °C	293	312.5	272	300	309	262	283	272	322	298	300
Tops-Bottom Split, %	16	46	45	18	5	8	5	10	38	33.8	44.5
Total Removal, %	36	81	81	59	18	22	18	23	54	54.2	72.1
Char pot loading	1.52%	1.08%	1.28%	2.98%	1.89%	1.81%	2.32%	1.17%	0.95%	1.65%	2.49%
Clean OC loading	0.50%	0.22%	0.25%	0.45%	0.52%	0.59%	0.61%	0.53%	0.49%	0.71%	0.80%



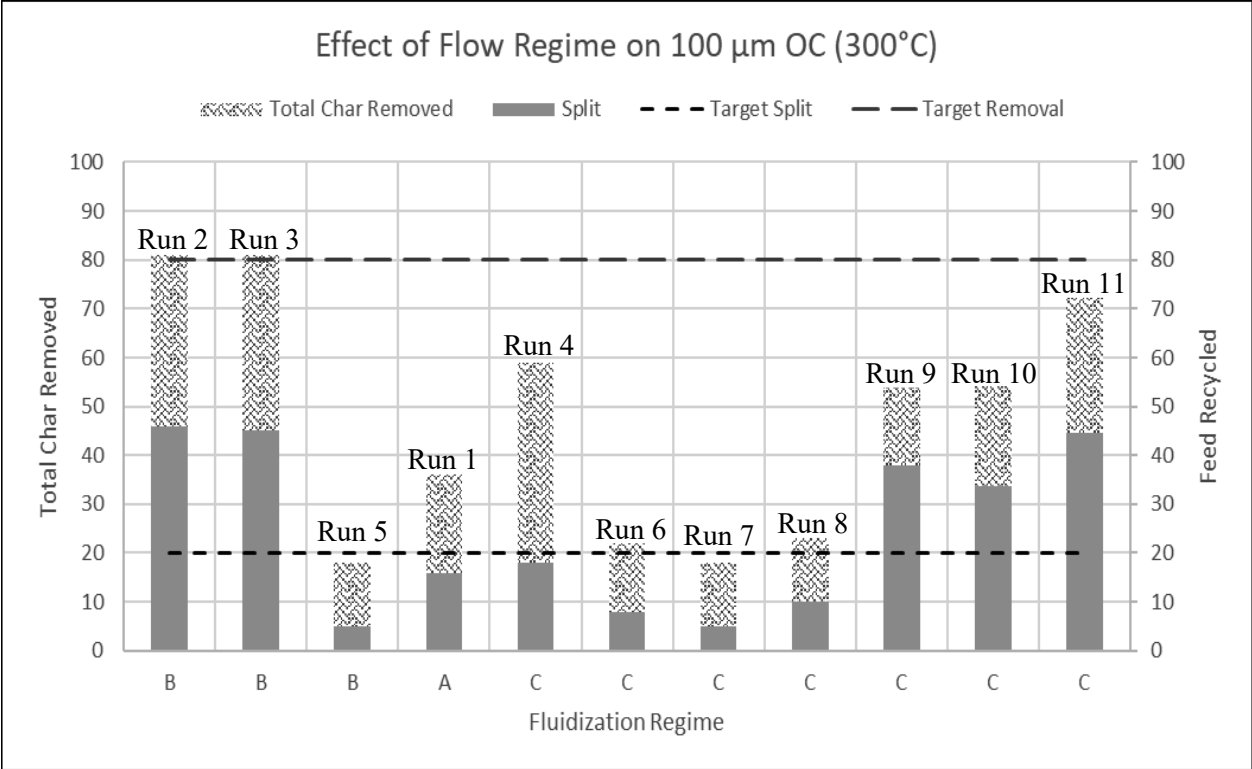


Figure 35. Char removal for 94 μm OC

## CHAPTER VI FUTURE WORK

The work scope of this project was to design, fabricate, and test a hot flow char separation system in order to identify optimum operating conditions. Additional work is continuing beyond the original thesis definition to help identify these conditions. Additional testing at ~ 300 °C will consist of testing higher average flow rates along with different fluidization regimes to see if they will result in better separation efficiency (high char removal with low split).

Upon completion of 300°C tests, the next step will be to perform temperature shakedown at 800°C. Tests will be performed to see if agglomeration of ilmenite occurs under varying conditions. Next, tests at 800°C will be performed to validate separation performance at actual CLC temperatures. Additionally, the coarse and fine batches of ilmenite will be mixed together to create varying particle size distributions that will be representative of different levels of attrition. This will show more accurately how separation is affected as ilmenite is cycled through a CLC system. Lastly, steam will be introduced to the SSB along with nitrogen to see how reacting conditions will affect separation of char from ilmenite.

## CHAPTER VII CONCLUSIONS

The objective of this project was to design and develop a system capable of separating unconverted fuel (char) from oxygen carriers in a chemical looping combustion system in order to achieve high carbon capture rates (CCR). The particle char separator (PCS) was developed and proof of concept testing showed promising results. During the design and construction phase challenges were addressed and a 50 kg/hr cold flow system was constructed in order to finalize the hot flow design. Following completion of cold flow testing, the 50 kg/hr hot flow system was successfully constructed and tested. After shakedown of the system, results from tests conducted at approximately 300°C demonstrated that temperature has no impact on the ability for the PCS to separate char from ilmenite. Best results to date show a char removal of 83% with a 32% recycle of ilmenite (split). This split was higher than the target (20%), however, results from the cold flow system show that higher separation efficiencies are likely achievable. Overall, the particle char separator (PCS) has proven to be capable of separating all size fractions of char and would be effective in achieving high carbon capture rates (CCR) when implemented into a CLC system.

## REFERENCES

- 1 Tans P. Trends in carbon dioxide. NOAA/ESRL. Available in:  
<http://www.esrl.noaa.gov/gmd/ccgg/trends/>.
- 2 IPCC special report on carbon dioxide capture and storage. Cambridge, UK: Cambridge University Press; 2005.
- 3 International Energy Agency (IEA). Energy technology perspectives: scenarios and strategies to 2050. Paris, France: OECD/IEA; 2006.
- 4 Müller CR, Brown TA, Bohn CD, Chuang SY, Cleeton JPE, Scott SA, et al. Experimental investigation of two modified chemical looping combustion cycles using syngas from cylinders and the gasification of solid fuels. Proc. 20th Int. Conf. on Fluidized Bed Combustion. Xian, China; 2009: 590-5.
- 5 Chuang SY, Dennis JS, Hayhurst AN, Scott SA. Development and performance of Cu-based oxygen carriers for chemical-looping combustion. Combust. Flame 2008;154:109-21.
- 6 Forero CR, Gayán P, García-Labiano F, de Diego LF, Abad A, Adánez J. CuO High temperature behaviour of a CuO/□Al<sub>2</sub>O<sub>3</sub> oxygen carrier for chemical looping combustion. Int. J. Greenhouse Gas Control 2011;5:659-67.

7 Adánez J, García-Labiano F, de Diego LF, Gayán P, Celaya J, Abad A. Nickel copper oxygen carriers to reach zero CO and H<sub>2</sub> emissions in chemical looping combustion. *Ind. Eng. Chem. Res.* 2006;45:2617-25.

8 U.S. Department of Energy, NETL. DOE/NETL Advanced Combustion Systems: Chemical Looping Summary. July 2013.

9 Bayham, S. C.; Kim, H. R.; Wang, D.; Tong, A.; Zeng, L.; McGiveron, O.; Kathe, M. V.; Chung, E.; Wang, W.; Wang, A.; Majumder, A.; Fan. L.-S., "Iron-Based Coal Direct Chemical Looping Combustion Process: 200-h Continuous Operation of a 25-kWth Subpilot Unit," *Energy Fuels* 27 (2013) 1347-1356.

10 Leion H, Mattisson T, Lyngfelt A. The use of petroleum coke as fuel in chemical-looping combustion. *Fuel* 2007;86:1947-58.

11 Shen L, Wu J, Xiao J, Song Q, Xiao R. Chemical-looping combustion of biomass in a 10 kW reactor with iron oxide as an oxygen carrier. *Energy Fuels* 2009;23: 2498-505.

12 Berguerand N, Lyngfelt A. Design and operation of a 10 kWth chemical looping combustor for solid fuels - Testing with South African coal. *Fuel* 2008;87:2713-26.

13 Berguerand N, Lyngfelt A. The use of petroleum coke as fuel in a 10 kW chemical-looping combustor. *Int. J. Greenhouse Gas Control* 2008;2:169-79.

14 Thon, A, et al., et al. 2014, *J. Applied Energy*, Vol. 118, pp. 309-317.

15 Operation of a 100 kW chemical-looping combustor with Mexican petroleum coke and Cerrejon coal. Markstrom, P, Linderholm, C and Lyngfelt, A. Darmstadt, Germany : 2nd International Conference on Chemical Looping, 2012.

- 16 Alstom's calcium oxide chemical looping combustion coal power technology development. E, Andrus H., et al., et al. Clearwater, Florida : International Technical Conference on Clean Coal & Fuel Systems, 2009.
- 17 Mattisson T, Johansson M, Lyngfelt A. CO<sub>2</sub> capture from coal combustion using chemical-looping combustion- Reactivity investigation of Fe, Ni and Mn based oxygen carriers using syngas. In: Proc. of the Clearwater Clean Coal Conf. Clearwater, Florida, USA; 2006.
- 18 Johansson M, Mattisson T, Lyngfelt A. Comparison of oxygen carriers for chemical-looping combustion of methane-rich fuels. In: Proc. 19th Int. Conf. on FBC. Vienna, Austria; 2006.
- 19 Abad A, Mattisson T, Lyngfelt A, Rydén M. Chemical-looping combustion in a 300 W continuously operating reactor system using a manganese-based oxygen carrier. Fuel 2006;85:1174-85.
- 20 Arjmand, M, et al., et al. s.l. : Applied Energy, 2014, Vol. 113, pp. 1183-1894.
- 21 Sun, H., Cheng, M., Chen, D., Xu, L., Li, Z., Cai, N. Ind. Eng. Chem. Res. **2015**, v. 54, pp. 8743–8753.
- 22 Sun, H., Cheng, M., Li, Z., Cai, N. Ind. Eng. Chem. Res. **2016**, v. 55, pp. 2381–2390
- 23 Ströhle, J., Orth, M., Epple, B. Applied Energy **2015**, v. 157, pp. 288-294
- 24 Abad, A., Adánez, J., Gayán, P., de Diego, L. F., García-Labiano, F., Sprachmann, G. Applied Energy **2015**, v. 157, pp. 462-474.
- 25 Markstrom, P., Linderholm, C., Lyngfelt, A. Int. J. of Greenhouse Gas Control **2013**, v.15, pp. 150-162.

- 26 Oxidation and Reduction of Iron-Titanium Oxides in Chemical Looping Combustion: A Phase-Chemical Description. Hoed, P. and Luckos, A. 2, 2011, Oil & Gas Science and Technology, Vol. 66, pp. 249-263.
- 27 The use fo ilmenite as an oxygen carrier in chemical-looping combustion. Leion, H., et al., et al. 9, September 2008, Chemical Engineering Research and Design, Vol. 86, pp. 1017-1026.
- 28 An Investigation Into the Operation of the Twin-Exit Loop-Seal of a Circulating Fluidized Bed Boiler in a Thermal Power Plant and its Design Implication. Basu, Prabir, et al., et al. 4, October 12, 2009, Journal of Energy Resources Technology, Vol. 131.
- 29 D. Kunii and O. Levenspiel, *Fluidization engineering*. Amsterdam: Elsevier, 2012.
- 30 Knight, J.B, Jaeger, H.M and Nagel, S. 1993, Physical Review Letters, Vol. 70, p. 3728.